

Mapping between finite temperature classical and zero temperature quantum systems: Quantum critical jamming and quantum dynamical heterogeneities

Zohar Nussinov,^{1,2} Patrick Johnson,¹ Matthias J. Graf,³ and Alexander V. Balatsky^{3,4}

¹*Department of Physics, Washington University, St. Louis, Missouri 63130, USA*

²*Kavli Institute for Theoretical Physics, Santa Barbara, California 93106, USA*

³*Theoretical Division, Los Alamos National Laboratory, New Mexico 87545, USA*

⁴*NORDITA, Roslagstullsbacken 23, 106 91 Stockholm, Sweden*

(Received 3 December 2012; published 15 May 2013)

Many electronic systems (e.g., the cuprate superconductors and heavy fermions) exhibit striking features in their dynamical response over a prominent range of experimental parameters. While there are some empirical suggestions of particular increasing length scales that accompany such transitions in some cases, this identification is not universal and in numerous instances no large correlation length is evident. To better understand, as a matter of principle, such behavior in quantum systems, we extend a known mapping (earlier studied in stochastic or supersymmetric quantum mechanics) between finite temperature classical Fokker-Planck systems and related quantum systems at zero temperature to include general nonequilibrium dynamics. Unlike Feynman mappings or stochastic quantization methods in field theories (as well as more recent holographic type dualities), the classical systems that we consider and their quantum duals reside in the same number of space-time dimensions. The upshot of our very broad and rigorous result is that a Wick rotation exactly relates (i) the dynamics in general finite temperature classical dissipative systems to (ii) zero temperature dynamics in the corresponding dual many-body quantum systems. Using this correspondence, we illustrate that, even in the absence of imposed disorder, many continuum quantum fluid systems (and possible lattice counterparts) may exhibit a zero-point “quantum dynamical heterogeneity” wherein the dynamics, at a given instant, is spatially nonuniform. While the static length scales accompanying this phenomenon do not seem to exhibit a clear divergence in standard correlation functions, the length scale of the dynamical heterogeneities can increase dramatically. We further study “quantum jamming” and illustrate how a hard-core bosonic system can undergo a zero temperature quantum critical metal-to-insulator-type transition with an extremely large effective dynamical exponent $z > 4$ that is consistent with length scales that increase far more slowly than the relaxation time as a putative critical transition is approached. Similar results may hold for spin-liquid-type as well as interacting electronic systems. We suggest ways to analyze experimental data in order to adduce such phenomena. Our approach may be used to analyze other quenched quantum systems.

DOI: [10.1103/PhysRevB.87.184202](https://doi.org/10.1103/PhysRevB.87.184202)

PACS number(s): 05.30.—d

I. INTRODUCTION

A prominent centerpiece in the understanding of numerous systems is Landau Fermi-liquid (LFL) theory; this theory allows the understanding of phenomena such as conventional metals and low-temperature ³He liquids. LFL theory is centered on the premise that the low-energy states of interacting electron systems may be captured by long-lived fermionic quasiparticles with renormalized parameters (e.g., effective masses that differ from those of the bare electron). The last three decades have seen the discovery of materials in which electronic behavior deviates from simple LFL-type behavior. These “singular” or “non-Fermi liquids” (NFL) include the pseudogap region of the high-temperature cuprate superconductors and “heavy fermions” (in which, as befits their name, the effective electron mass becomes very large). While there are clear indications of changes in the dynamics in these systems, including putative quantum critical points,^{1,2} there is, in most cases, no clear experimentally measured length scale that exhibits a clear divergence. A quantum critical point is associated with a continuous phase transition at (absolute) zero temperature. Typically, this may occur in a system whose transition temperature is driven to zero by doping or the application of magnetic fields or pressure. Within a quantum critical regime, response functions follow universal power-law scaling in both space and time. Specifically, at a

quantum critical point, the effective infrared (IR) fixed point theory exhibits scaling invariance in space-time: $t \rightarrow \lambda t, \vec{x} \rightarrow \lambda^{1/z} \vec{x}$ with a dynamical exponent z that can, depending on the theory at hand, assume various canonical values. Unlike classical critical points whose associated critical fluctuations are confined to a narrow region near the phase transition, quantum critical fluctuations appear over a wide range of temperatures above the quantum critical point. These fluctuations may generally lead to a radical departure of the system’s electronic properties from standard LFL-type behavior. These features are anticipated to be common across many strongly correlated electronic systems and may be associated, in some electronic systems, with a change of Fermi-surface topology.³ The genesis of NFL behavior in myriad systems has attracted much attention. Various theoretical proposals for quantum critical points in NFL include, amongst many others, those that raise the specter of distinct local quantum critical points⁴ of specific types, e.g.,⁵ as well as new special topological excitations.⁶ In this work, we wish to suggest that some aspects of effectively local behaviors exhibited by many strongly correlated electronic systems might rather be understood as direct quantum renditions of known classical behaviors that naturally appear over a broad range of parameters. Quantum spin (or other) systems may display⁷ exotic properties such as those associated with fractionalization

at deconfined critical points that ultimately reflect classical transitions

Many non-Fermi Liquids exhibit numerous phases (including, quite notably, superconductivity). Indeed, competing orders and proliferation of multiple low-energy states can lead to spatially nonuniform glassy characteristics⁸ and associated first-order quantum transitions.⁹ The length scales characterizing these electronic systems undergo a much milder change than the corresponding changes in the dynamics. All of this suggests an effective infrared (IR) fixed point quantum field theory which is invariant under scaling in time but not in space, i.e., the effective dynamical exponent $z \rightarrow \infty$. Response functions such as those of the marginal Fermi-liquid form² describing cuprates near optimal doping show a marked frequency dependence but essentially no spatial momentum dependence. In this work, we will suggest how many quantum systems might exhibit very large effective dynamical exponents.

It is natural to first look elsewhere in physics where similar phenomena appear. One arena immediately comes to mind. In classical structural glasses, there is a dramatic change in the dynamics as a liquid is rapidly cooled (supercooled) below its melting temperature, it falls out of equilibrium at low temperatures and becomes quenched into a glass without the appearance of easily discernible large changes in measurable standard static length scales. While the ergodicity breaking that accompanies a glass transition can not occur in a finite-size system, it essentially mandates the appearance of a diverging static length scale,¹⁰ but such divergent length scales generally do not simply manifest themselves in bare standard correlation functions. General correlation functions which may monitor subtle changes include the “point-to-set”¹¹ correlations and others. Practically, in most instances,¹² no clear signatures of divergent length scales are easily seen in standard static two-point correlation functions.

A far more transparent growth in length scales is seen from four-point correlation functions that quantify the change in correlations as the system evolves in time. These correlation functions afford a glimpse into the length and time scaling which describe dynamical heterogeneities that characterize the spatially nonuniform rate of change or dynamics in the system. The length scale associated with these heterogeneities was seen to grow as the characteristic relaxation times increased.

We may use similar correlation functions to characterize strongly correlated electronic systems in which there are strongly discernible changes in the dynamics but no obvious experimentally accessible tools that point to accompanying divergent length scales in a general way.¹³ To our knowledge, to date, dynamical heterogeneities (or general static measures such as those of the point-to-set method) have not been systematically probed in electronic systems nor has their existence been established as a matter of principle in quantum systems. Initial ideas concerning nonuniform doping-driven heterogeneities were discussed in Ref. 14. In this work, we flesh out the blueprint for a proof outlined, by one of us, in Ref. 15 and we will provide concrete “matter of principle” theoretical testimony to the emergence of quantum dynamical heterogeneities in *clean systems* and related properties in quantum many-body systems. Some time after Ref. 15, the authors of Ref. 16 have further confirmed the existence of quantum dynamical heterogeneities in certain dissipative spin

systems. In what follows, we focus on systems such as structural glasses or jammed systems with no external disorder.

As is well appreciated, such translationally invariant systems that are free of external disorder may, on their own, display nonuniform spatial patterns concomitant with interesting dynamical properties.¹⁷ For times far shorter than the equilibration times, the two-point auto-correlation function

$$C(\vec{x}, t) = \langle \delta\phi(\vec{x}, t) \delta\phi(\vec{x}, 0) \rangle, \quad (1)$$

with the brackets denoting an average over a translationally invariant equilibrium average, records dynamic fluctuations at all points \vec{x} in d -dimensional space. In Eq. (1), the (deviations of the) fields $\delta\phi(\vec{x}, t)$ may correspond to, e.g., density or any other pertinent spatiotemporal quantity characterizing the system. A notable variant in classical liquids is that for the mobility field where, in all correlators, $\delta\phi(\vec{x}, t)$ is replaced by

$$\mu(\vec{x}, t) = \sum_{i=1}^N w_i(t) \delta[\vec{x} - \vec{x}_i(0)], \quad (2)$$

with an individual particle (i) mobility w_i monitoring particle motion during a time interval of size t , e.g., $w_i(t) = \exp[-|\vec{r}_i(t) - \vec{r}_i(0)|^2/d^2]$ with d the particle size. The two-point correlator of Eq. (1) constitutes an analog of the Edwards-Anderson¹⁸ order parameter that appears in spin glasses. In uniform systems, the correlator of Eq. (1) is spatially (\vec{x}) independent. The spatial correlation amongst pair products of time-separated products of fields [such as those in Eq. (1)] at different spatial sites is a four-point correlation function¹⁹ that attempts to measure cooperation

$$G_4(\vec{x} - \vec{y}, t) = \langle \delta\phi(\vec{x}, t) \delta\phi(\vec{x}, 0) \delta\phi(\vec{y}, t) \delta\phi(\vec{y}, 0) \rangle - C(\vec{x}, t) C(\vec{y}, t). \quad (3)$$

This four-point correlation function relates the dynamics at two different spatial points \vec{x} and \vec{y} . Generally, in the absence of quenched disorder, due to translational invariance, this correlation function depends only on $(\vec{x} - \vec{y})$ and not on \vec{x} and \vec{y} separately. Empirically, the integral of this correlation function,

$$\chi_4(t) = \int d^d x G_4(\vec{x}, t) = \langle \tilde{C}^2(t) \rangle - \langle \tilde{C}(t) \rangle^2, \quad (4)$$

where $\tilde{C}(t) = \int d^d x \delta\phi(\vec{x}, t) \delta\phi(\vec{x}, 0)$ [or, correspondingly, $\tilde{C}(t) = \int d^d x \mu(\vec{x}, t) \mu(\vec{x}, 0)$ for spatiotemporal correlations of the mobility of Eq. (2)] is often employed to enable a quantification of dynamical heterogeneities when the atomic coordinates may be resolved.¹⁷

II. OUTLINE

This paper illustrates that the above-mentioned zero-point dynamical heterogeneities can indeed rear their head in quantum many-body systems. It more rigorously shows that zero temperature quantum many-body systems can, apart from quantum critical phenomena,^{1,2} exhibit exact analogs of finite temperature classical behavior including that in glass-forming systems. Towards this end, we establish two sets of results:

(1) Simple mathematical relations between the dynamical correlation functions in (different) classical and quantum

systems when these systems are linked to one another by a duality that we will describe.

(2) Physical consequences of these mathematical relations when these are applied to classical glass-forming systems (whence they lead to predictions for the zero temperature time-dependent correlation functions in dual quantum systems).

Accordingly, our work is split into, roughly, two equal parts describing physical background and derivations that realize both of these endeavours. The outline of this paper is as follows. In Sec. III, we establish our main result given by Eq. (9), which links time-dependent correlation functions in finite temperature dissipative classical systems with their dual zero temperature quantum systems. After stating our result, much time is spent deriving it from first principles. Towards this end, we first review the rudiments of stochastic quantum mechanics and then derive in detail the key result in Eq. (9) and similar relations like it for higher-order correlations. In Sec. IV, we explicitly list several (of the many) dissipative classical systems that exhibit dynamical heterogeneities and other facets of glassy dynamics and their quantum duals.

With these relations in tow, we then proceed to discuss physical predictions for quantum many-body systems. In Sec. V, we establish the existence of quantum dynamical heterogeneities, scaling of relaxation times, and quantum critical jamming. In the quantum dual models that exhibit these phenomena, the relaxation times increase much more rapidly than correlation length scales. Further building on these results, in Secs. VI and VII we introduce hard-core Bose systems as well as electronic systems with pairing interactions that may display glassy dynamics. We outline in Sec. VIII data analysis that may validate the presence of quantum dynamical heterogeneities in experimental systems. We conclude (Sec. IX) with a synopsis of our central results. Several technical details have been relegated to the Appendices [including, perhaps most notably (Appendix A) the proper analytic continuation for stretched exponential dynamical correlations in dissipative classical systems to obtain correlations in the corresponding quantum glass systems].

III. A DYNAMICAL RELATION BETWEEN VISCOUS CLASSICAL AND QUANTUM MANY-BODY SYSTEMS

In order to illustrate how, as a matter of principle, the physics of such classical dissipative systems can appear in clean quantum systems at zero temperature, we employ and extend a mapping^{20–28} between classical dissipative systems and quantum many-body systems to include general dynamical (including nonequilibrium) systems. Aspects of this mapping are intimately linked to Madelung hydrodynamics²⁹ which links the real and imaginary parts of the Schrödinger equation to classical hydrodynamics. Related work concerning dynamics in Rokhsar-Kivelson³⁰ systems also appears in Ref. 31. In the following, we first briefly review this mapping. We will then derive a hitherto unknown result linking the dynamics in these classical and quantum systems. In these and other calculations, we employ units in which both Boltzmann's constant and the reduced Planck constant are set to unity, $k_B = \hbar = 1$.

The crux of the “stochastic quantum mechanics” mapping between dissipative classical systems and many-body bosonic

theories^{20–28} is the realization that the equation of motion for a dissipative (or “Aristotelian”) classical system is a first-order differential equation in time just as the Schrödinger equation is. Using this equivalence, systems obeying the Langevin equation

$$\gamma_i \frac{d\vec{x}_i}{dt} = -\vec{\nabla}_i V_N(\vec{x}_1, \dots, \vec{x}_N) + \vec{\eta}_i(t), \quad (5)$$

with i the particle index, γ_i the coefficients of friction, $\eta_i^\alpha(t)$ Cartesian components of the Gaussian noise at site i with

$$\langle \eta_i^\alpha(t) \eta_j^\beta(t') \rangle = 2T_{cl} \gamma_i \delta_{ij} \delta_{\alpha\beta} \delta(t - t'), \quad (6)$$

where T_{cl} is the effective temperature of the classical system, and $\alpha, \beta = 1, 2, \dots, d$ (with d the system dimensionality) can be exactly mapped^{20,21,26} onto a quantum many-body system of bosons with effective mass $m_i = \gamma_i / (2T_{cl})$ at zero temperature, which is governed by the Hamiltonian

$$\begin{aligned} H &= \sum_i \frac{1}{\gamma_i} \left[-T_{cl} \nabla_i^2 - \frac{1}{2} \nabla_i^2 V_N + \frac{1}{4T_{cl}} (\nabla_i V_N)^2 \right] \\ &\equiv \sum_i \frac{p_i^2}{2m_i} + \mathcal{V}_{\text{Quantum}}(\{\vec{x}\}). \end{aligned} \quad (7)$$

We will term the quantum system of Eq. (7) “the dual quantum system” associated with the classical system of Eqs. (5) and (6). The many-body quantum potential $\mathcal{V}_{\text{Quantum}}(\{\vec{x}\})$ is constructed from the gradients of the classical potential energy V_N as in Eq. (7). Under this mapping,^{20–25} a dissipative classical system with a potential energy V_N that captures *repulsive hard-core spheres* maps onto a quantum system at zero temperature with (as is apparent in the many-body potential energy $\mathcal{V}_{\text{Quantum}}$) similar *dominant hard-core interactions* (augmented by soft sticky interactions).²⁶ Although we will focus on the mapping from classical systems to corresponding quantum ones, it is also possible to go in the opposite direction and map quantum mechanical systems with known nondegenerate ground states onto classical dissipative systems (see Appendix E). (For completeness, we note that different “stochastic quantization”³² mappings relate stochastic systems to quantum field theories by the introduction of an additional fictitious time coordinate. An additional timelike coordinate also appears in well-known textbook-type Feynman mapping as well as far more recent holographic dualities.³³ By contrast, in the “stochastic quantum mechanics” mappings between classical to quantum systems that we review and expand on here to generally include dynamics, the number of space-time dimensions is identical.)

Earlier work^{20–26} advanced the rudiments of this mapping and further suggested dynamical aspects that might follow from it. In this work, we explicitly derive and prove a general and rather powerful relation between arbitrary correlation functions in dissipative classical systems with time-varying potentials (necessary for our discussion of quenching) and relate these to corresponding correlation functions in zero temperature quantum systems. In Sec. III B, we summarize, following Refs. 20 and 22–26, more detailed aspects of this mapping. We now proceed to set the stage for our result and its consequences. In what follows, we consider a general classical

two-point correlation function of the form

$$G_{\text{classical}}(t) = \langle \mathcal{O}(t)\mathcal{O}(0) \rangle, \quad (8)$$

where $\mathcal{O}(t)$ is *any* quantity, at times $t \geq 0$. Our mapping covers general nonequilibrium time-dependent Hamiltonians in which only the initial (or only the final) classical system is in thermal equilibrium at an initial (or final) temperature. In such a case, the corresponding dual quantum problem evolves unitarily with a time-dependent Hamiltonian. Specifically, as we will elaborate on in Sec. III B, we find a very simple and general result for *any* quantity $\mathcal{O}(t)$:

$$G_{\text{Quantum}}(t) = G_{\text{classical}}(it). \quad (9)$$

Thus, a ‘‘complexification’’ of the time coordinate (or *Wick-type rotation*) relates general classical dynamical correlation functions of the form of Eq. (8) to their corresponding quantum counterparts. The quantum correlation function $G_{\text{Quantum}}(\vec{q}, t)$ is evaluated with the quantum many-body potential $\mathcal{V}_{\text{Quantum}}(\{\vec{x}\})$ of Eq. (64), while the corresponding classical correlation function is computed for a system with a potential $V_{\text{N}}(\{\vec{x}\})$. Similarly, for the quantum linear response functions $R_{\text{Quantum}}(t)$ [see Eqs. (58) and (59) for standard linear response expressions], we have that

$$R_{\text{Quantum}}(t) = i\Theta(t)[G_{\text{classical}}(it) - G_{\text{classical}}^*(it)]. \quad (10)$$

Equations (9) and (10) provide an entry in the mapping between the finite temperature classical system of Eq. (5) governed by a potential V_{N} and its corresponding quantum zero temperature dual with a quantum many-body potential energy $\mathcal{V}_{\text{Quantum}}(\{\vec{x}\})$ in the Hamiltonian of Eq. (7).

Equations (9) and (10), along with their consequences, are key results of this work. In Sec. III B, we provide a detailed derivation of Eqs. (9) and (10). Typically, in glassy systems, the correlation function of Eq. (8) is a superposition of many decaying modes. This distribution of modes will manifest itself as a distribution of oscillatory modes in the corresponding dual quantum problem. In many cases, this will lead to zero temperature quantum dynamics of the dual system that, with additional oscillations, will emulate the finite classical dynamics. For instance, as it precisely occurs in viscous systems with overdamped dynamics [for which Eq. (5) applies], if for times $t > 0$,

$$G_{\text{classical}}(t) = A \exp[-(t/\tau)^c], \quad (11)$$

then, correspondingly for all of these positive times t (see Appendix A),

$$R_{\text{Quantum}}(t) = 2Ae^{-\left(\frac{t}{\tau}\right)^c \cos \frac{\pi c}{2}} \sin \left[\left(\frac{t}{\tau}\right)^c \sin \frac{\pi c}{2} \right]. \quad (12)$$

With the aid of the general relation of Eqs. (9) and (10), the quantum correlation function that corresponds to a general stretched exponential correlation function in the classical arena can be computed analytically. The linear response function is, indeed, given by Eq. (12). A trivial yet important particular corollary of Eq. (9) is that static correlations (i.e., those for $t = 0$) are identical in the finite temperature classical and their corresponding quantum dual systems.

The remainder of this section is organized as follows. In Sec. III A, we review the basic known essentials of the mapping

between finite temperature classical dissipative systems and their quantum duals. This is then followed, in Sec. III B, by the derivation of our result of Eq. (9).

A. Lightning review of known relations in stochastic quantum mechanics

This section reviews earlier work which is necessary for our derivations in the sections that follow. We will now briefly highlight known salient features of the mapping^{20–26} between classical stochastic systems and their quantum duals (aka ‘‘stochastic quantum mechanics’’). The subsections (and sections) that follow will build on the classical to quantum mapping that we now discuss here. There are two prominent independent approaches that establish this duality: (i) a general method that examines the Fokker-Planck equations and (ii) an algebraic method highlighting a harmonic oscillator (with a simple raising/lowering operator) type structure akin to that more generally found in supersymmetric theories. Both approaches directly lead to the effective quantum Hamiltonian of Eq. (7). Although this Hamiltonian is more readily seen in the algebraic formulation and leads to immediate and clear intuition (which is why we briefly review it), the broader approach is arguably that relying on the direct Fokker-Planck evolution of dissipative classical systems. It is this Fokker-Planck approach that we will use in our derivations in the subsections that follow.

1. Fokker-Planck systems and their quantum duals

We first set the preliminaries for the Fokker-Planck approach following Ref. 21. Given an initial vector x_0 of the coordinates of all particles at time $t = t_0$, the time-dependent probability distribution $\mathcal{P}(\vec{x}, t; \vec{x}_0, t_0)$ for the corresponding position vectors $\{\vec{x}(t)\}$ at time t is given by

$$\mathcal{P}(\{\vec{x}\}, t; \{\vec{x}_0\}, t_0) = \left\langle \prod_{i=1}^N \delta[\{\vec{x}_i(t) - \vec{x}_i\}] \right\rangle_{\{\vec{\eta}\}, \{\vec{x}_0\}}, \quad (13)$$

where $\langle \dots \rangle_{\eta, \{\vec{x}_0\}}$ denotes the average over the random noise η [which we will take to be the Gaussian white noise of Eq. (6)] given that initially, at time $t = t_0$, the particle coordinates were $\{\vec{x}_0\}$. The average of a general function $\mathcal{O}[\{\vec{x}(t)\}]$ is then

$$\int d^{dN} x \mathcal{P}(\{\vec{x}\}, t; \{\vec{x}_0\}, t_0) \mathcal{O}(\{\vec{x}\}) = \langle \mathcal{O}(\{\vec{x}(t)\}) \rangle_{\{\vec{\eta}\}, \{\vec{x}_0\}}. \quad (14)$$

It is convenient to write $\mathcal{P}(\{\vec{x}\}, t; \{\vec{x}_0\}, t_0)$ in a Dirac notation as

$$\mathcal{P}(\{\vec{x}\}, t; \{\vec{x}_0\}, t_0) = \langle \{\vec{x}\} | \hat{P}(t, t_0) | \{\vec{x}_0\} \rangle. \quad (15)$$

Time translation invariance and the Markov property of these probabilities,

$$\begin{aligned} & \int d^{dN} x' \langle \{\vec{x}\} | \hat{P}(t, t') | \{\vec{x}'\} \rangle \langle \{\vec{x}'\} | \hat{P}(t', t_0) | \{\vec{x}_0\} \rangle \\ &= \int d^{dN} x' \mathcal{P}(\{\vec{x}\}, t; \{\vec{x}'\}, t') \mathcal{P}(\{\vec{x}'\}, t'; \{\vec{x}_0\}, t_0) \\ &= \mathcal{P}(\{\vec{x}\}, t; \{\vec{x}_0\}, t_0), \end{aligned} \quad (16)$$

imply that

$$\hat{P}(t, t_0) = \mathcal{T} e^{-\int_{t_0}^t H_{FP}(t') dt'}, \quad (17)$$

with a ‘‘Fokker-Planck’’ Hamiltonian H_{FP} and where \mathcal{T} is the time-ordering operator. We now return to our particular classical-to-quantum mapping. The summary below closely follows this mapping as presented by Biroli *et al.*²⁶ In what follows, we set

$$P = \hat{P}(t, t_0) | \{ \vec{x}_0 \} \rangle. \quad (18)$$

For the classical dissipative system of Eq. (5), the probability distribution $P(\{ \vec{x} \})$ evolves according to the Fokker-Planck equation

$$\frac{\partial P}{\partial t} = -H_{\text{FP}} P, \quad (19)$$

where the Fokker-Planck operator is

$$H_{\text{FP}} = - \sum_i \frac{1}{\gamma_i} \vec{\nabla}_i \cdot [\vec{\nabla}_i V_{\text{N}} + T_{cl} \vec{\nabla}_i], \quad (20)$$

with T_{cl} being the temperature of the classical system [setting the noise strength in Eq. (6)]. Equation (20) follows from a direct differentiation of Eq. (13) while invoking Eq. (5) for the derivatives of the coordinates $\{ \vec{x}_i(t) \}$ in the argument of the delta functions and performing short-time averages. (Thus, this equation and our results pertain to systems in which the dynamics is sufficiently slow such that short-time averages over the noise η at fixed temperature are sensible.) A detailed derivation of the Fokker-Planck equation for this and more general Langevin processes appears in many excellent textbooks, e.g., Ref. 34. The operator H_{FP} is non-Hermitian. Each eigenvalue is generally associated with differing left and right eigenvectors. The Fokker-Planck equation can be mapped into a Hermitian Hamiltonian by³⁵

$$H = e^{V_{\text{N}}/(2T_{cl})} H_{\text{FP}} e^{-V_{\text{N}}/(2T_{cl})} \quad (21)$$

if the second derivatives are exchangeable, $\vec{\nabla}_i \vec{\nabla}_j V_{\text{N}} = \vec{\nabla}_j \vec{\nabla}_i V_{\text{N}}$.³⁶ A direct substitution leads to the quantum many-body Hamiltonian of Eq. (7). Note that, thus far, we have allowed V_{N} to be completely general. This potential energy may include one-body interactions (i.e., coupling to an external source), pair interactions between particles, and three- and higher-order particle interactions. A key point that we will further invoke later is that the transformation of Eq. (21) leading to a Hermitian quantum Hamiltonian can be trivially performed at any given time slice when V_{N} and T_{cl} are, generally, time dependent. It is worth highlighting that in nonequilibrium time-dependent classical systems, the temperature T_{cl} is set by the time-dependent noise amplitude [following Eq. (6)]. For general $V_{\text{N}}(\{ \vec{x} \})$, the Fokker-Planck operator of Eq. (20) has non-negative eigenvalues.^{20,21} For any time-independent H_{FP} , the zero eigenvalue state, i.e., the ground state, which according to Eq. (19) corresponds to a stationary (time-independent) probability distribution P . This is the equilibrium Boltzmann distribution

$$P^{\text{equil}}(\{ \vec{x} \}, t) = \frac{1}{Z_{\text{N}}} e^{-\beta V_{\text{N}}(\{ \vec{x} \})}, \quad (22)$$

with Z_{N} the partition function associated with $V_{\text{N}}(\{ \vec{x} \})$ and $\beta = 1/T_{cl}$. This is readily rationalized by the following argument. For a finite-size system, the linear eigenvalue equation

$$(H_{\text{FP}})_{bc} P_c = -\varepsilon_c P_c, \quad (23)$$

with the matrix row/column indices b and c denoting classical configurations, has a (finite-size) matrix H_{FP} with positive off-diagonal elements and negative diagonal entries. Specifically, in Eqs. (19) and (23), the transition matrix H_{FP} has entries that relate the probabilities of going from state b to state c in a given (infinitesimal) time interval. If these states are different ($b \neq c$), then clearly $(H_{\text{FP}})_{bc} > 0$. The diagonal elements $(H_{\text{FP}})_{bb}$ provide the probabilities of ‘‘leaking out’’ of state b and going to all other states $c \neq b$. From all of this it follows that

$$(H_{\text{FP}})_{bb} = - \sum_{b' \neq b} (H_{\text{FP}})_{bb'} < 0. \quad (24)$$

Detailed balance, i.e., the fact that the probability of going from b to c is the same as that of going from c to b , asserts that

$$(H_{\text{FP}})_{bc} e^{-\beta E_b} = (H_{\text{FP}})_{cb} e^{-\beta E_c}. \quad (25)$$

Equations (23) and (25) illustrate that the Hamiltonian of Eq. (21) is Hermitian. In this classical system of Eq. (5), the energies of the classical states E_c are simply given by $V_{\text{N}}(\{ \vec{x} \})$ evaluated for the classical configurations c . With the aid of Eqs. (24) and (25), it is easy to see that the column vector $P_c^{\text{equil}} = Z_{\text{N}}^{-1} \exp(-\beta E_c)$ [i.e., the distribution of Eq. (22)] is a null eigenvector of Eq. (23). This probability eigenvector corresponds, of course, to the equilibrium Boltzmann distribution. The factor of Z_{N}^{-1} is inserted to ensure normalization of the classical probabilities (for any eigenstate): $\sum_c P_c = 1$. Now, we can add a constant to the finite-dimensional matrix

$$H_{\text{FP}} \rightarrow H_{\text{FP}} - \text{const} \equiv H'_{\text{FP}} \quad (26)$$

to generate a matrix $(-H'_{\text{FP}})$ that has all of its elements positive $(-H'_{\text{FP}})_{bc} > 0$. Specifically, to this end, in Eq. (26) we can choose const to be any constant larger than the sign inverted smallest off-diagonal element of $(-H_{\text{FP}})$, i.e., $\text{const} > -\min_{b \neq c} \{ (H_{\text{FP}})_{bc} \}$. For such a positive matrix, we can apply the Perron-Frobenius theorem which states that the largest eigenvector of $(-H'_{\text{FP}})$ is nondegenerate and that the eigenvector is the only eigenvector that has all of its elements positive with all other orthogonal eigenvectors having at least one negative element. Clearly, all of the eigenvectors of H_{FP} and H'_{FP} are identical with the corresponding eigenvectors of both operators merely shifted uniformly by a constant. With all of the above in tow, we see that P^{equil} corresponds to the largest eigenvector of $(-H'_{\text{FP}})$ and is thus also the largest eigenvector of $(-H_{\text{FP}})$. For a time-independent H_{FP} , as P^{equil} was the null eigenvector of H_{FP} , it follows that all other eigenvalues of Eq. (23), $\varepsilon > 0$, are positive and, according to Eq. (19) and explicit earlier discussions, evolve with time as $\lim_{t \rightarrow \infty} \exp(-\varepsilon t) = 0$. Thus, physically (as to be expected) at long times the system attains its equilibrium configuration of P^{equil} . In the corresponding zero temperature quantum problem, the dominant classical equilibrium state with a lowest energy. We will thus label it in Sec. III B by $|G\rangle$. The transformation of Eq. (21) relates the operators in the classical Fokker-Planck and zero temperature quantum problem to one another. The transformation for the right eigenvectors P of H_{FP} , which we explicitly denote below as $|-\rangle_{\text{FP}}$, to the eigenvectors of the quantum Hamiltonian H is trivially

$$|-\rangle_{\text{FP}} \rightarrow \exp[-V_{\text{N}}/(2T_{cl})] |-\rangle_{\text{FP}} = |-\rangle_{\text{Quantum}}. \quad (27)$$

Similarly, the left eigenvectors ($\langle -|_{\text{FP}}$) of H_{FP} are to be multiplied by $\exp[V_{\text{N}}/(2T_{\text{cl}})]$ in order to pass to the left eigenstates of the quantum problem. (In the quantum problem defined by H , the left and right eigenstates are trivially related to each other by Hermitian conjugation.) Applying Eq. (27) to the null right eigenstate of the Fokker-Planck Hamiltonian of Eq. (22), we see that the quantum eigenstate of H corresponding to this classical equilibrium state is given by

$$\Psi_0(\{\vec{x}\}) = \frac{1}{\sqrt{Z_{\text{N}}}} \exp\left(-\frac{1}{2T_{\text{cl}}} V_{\text{N}}(\{\vec{x}\})\right). \quad (28)$$

The prefactor in Eq. (28) is set by the normalization of this quantum state. When comparing Eqs. (22) and (28) to one another, we see that this wave function is related to the classical equilibrium probability eigenvector by the appealing relation $\Psi_0(\{\vec{x}\}) = \sqrt{P^{\text{equil}}(\{\vec{x}\})}$. When $V_{\text{N}}(\{\vec{x}\})$ is symmetric under the interchange of particle coordinates, the resulting wave function *may describe bosons*. For two-body interactions V_{ij} [Eq. (62)] that are symmetric under the permutations of i with j , the wave function of Eq. (28) is symmetric under any permutations of the particles. Thus, the ground-state wave function of Eq. (28) is a Jastrow-type wave function describing a bosonic system. Of course, generally, $V_{\text{N}}(\{\vec{x}\})$ can include not only two-body terms but also single-body contributions (local chemical potentials or fields) as well as three- and higher-body interactions. Although obvious, it is worth noting that if $V_{\text{N}}(\{\vec{x}\})$ (and thus the quantum Hamiltonian H) is invariant under any pairwise permutation P_{ij} , i.e., if $[H, P_{ij}] = 0$ then the symmetry of the initial wave function Ψ_0 (corresponding to the classical Boltzmann distribution for a system initially at an equilibrium at temperature T_{cl}) does not change as the system evolves with time (including general arbitrary H corresponding to classical variations in temperature and other parameters).

We next briefly discuss a generalization of Eq. (21). It is, of course, possible to write a general similarity transformation

$$H' = \tilde{S}^{-1} H_{\text{FP}} \tilde{S}, \quad (29)$$

with a time-dependent operator \tilde{S} . Under Eq. (29), the Fokker-Planck equation of Eq. (19) reads as

$$\partial_t \Psi = -H' \Psi, \quad (30)$$

where $\Psi = \tilde{S}^{-1} P$ with P given by Eq. (18).

2. An algebraic approach relating the ground state of a dual quantum system to the Boltzmann distribution of a finite temperature classical system

As is well known, there exists a beautiful link between stochastic classical statistical mechanics and supersymmetric quantum systems, e.g., Ref. 37. This connection is especially immediate for the ground-state wave functions which are of zero energy [as indeed that of Eq. (28)]. This might lead to the impression that the results that we will derive using the correspondence between classical dissipative systems and quantum duals are rather limited and special. Informally, this suggested by some to lead to un-normalizable wave functions if nonconstant equilibrium classical states are considered. As we will explicitly elaborate in Sec. III B, the time evolution operator $\mathcal{U}(t)$ in the corresponding dual quantum problem is

unitary and thus if an initial state is normalized [such as that of Eq. (28) corresponding to an initial classical equilibrium state], then the quantum state will remain normalized at all positive times [and vice versa for a unitary evolution towards a final state of the form of Eq. (28)]. Although the ground state of the quantum problem may be dismissed as trivial and special, the relations concerning the time evolution to states that are not of the form of Eq. (28) are not as immediate. These relations concerning the dynamics form the core of this work. For pedagogical purposes, we very briefly review here some central notions concerning the mapping of the Fokker-Planck process to supersymmetric quantum mechanics as they, in particular, pertain to the equilibrium problem. The explicit use of supersymmetry will not be invoked in the following and the discussion will be made as simple as possible. The Hamiltonian of Eq. (7) can, for fixed $\gamma_i = \gamma$ in a simple (single-particle) one-dimensional rendition which we adopt for ease of notation, be written as

$$H = \frac{T_{\text{cl}}}{\gamma} A^\dagger A, \quad (31)$$

where

$$A^\dagger = -\frac{\partial}{\partial x} + \frac{V'}{2T_{\text{cl}}}, \quad A = \frac{\partial}{\partial x} + \frac{V'}{2T_{\text{cl}}}. \quad (32)$$

In the higher-dimensional many-body problem, the gradients are relative to each of the Cartesian coordinates of all of the particles and V is replaced by $V_{\text{N}}(\{\vec{x}\})$. Clearly, $\gamma A^\dagger A \geq 0$ and thus if a zero-energy eigenstate of H can be found, it is the ground state. Now, the square root of the classical equilibrium distribution function, i.e., the wave function of Eq. (28), is clearly a null eigenstate of the operator A above. Inserting Eq. (32) into Eq. (31) leads to the identification of the quantum many-body potential in terms of the corresponding classical potential energy $V_{\text{N}}(\{\vec{x}\})$. The astute reader will, up to trivial alterations, recognize these operators as the standard raising and lowering operators of the harmonic problem when V is a harmonic potential. We briefly return to this point in Sec. III C 3. The basic general relation between quantum and classical systems for wave functions of the eikonal type is further discussed in Appendix B. We provide very simple illustrative examples of the duality in Appendix C.

B. Derivation of the quantum-to-classical correspondence for general dynamical correlation functions

The central role of this section is the derivation of Eqs. (9) and (10) [or, more precisely, the derivation of Eqs. (49) and (50) that will lead to Eqs. (9) and (10)]. The sole assumption made in the following derivation of Eqs. (49) and (50) is that the classical system starts from its equilibrium state and then evolves with some general (time-dependent) potential $V_{\text{N}}(t)$. This will be mapped onto analytic continuations of the correlation and response functions of a quantum system that starts at time $t = 0$ in its ground state of Eq. (28) and then evolved with the corresponding (time-dependent) Hamiltonian $H(t)$. It is important to emphasize that we make no assumptions regarding the final (and intermediate) states. The classical (quantum) system need not stay in equilibrium (or within a ground state) as it evolves in time. Before detailing the derivation, we collect the basic relations discussed in Sec. III A with several new

definitions:

$$P(\{x\},t) = \langle \{x\} | P(t) \rangle, \quad (33)$$

$$P_G(\{x\},t) = \langle \{x\} | G \rangle = \frac{e^{-V_N(\{x\})/T_{cl}}}{Z_N}, \quad (34)$$

$$H_{FP}|G\rangle = 0, \quad (35)$$

$$\langle + | \{x\} \rangle = 1, \quad (36)$$

$$H = e^{V_N/2T_{cl}} H_{FP} e^{-V_N/2T_{cl}}. \quad (37)$$

These will serve as a point of departure for the calculations in this section. Equation (33) represents a general probability distribution in bra-ket notation. Equation (34) defines the ground-state distribution as a Boltzmann distribution in bracket notation. Equation (35) defines the ground state as the eigenvector of the Fokker-Planck Hamiltonian with zero eigenvalue. Equation (36) defines the state $|+\rangle$ to be the uniform state such that $|+\rangle = \int d\{x\} |+\rangle$. Lastly, Eq. (37) can be used to find a relationship between H_{FP} and H_{FP}^\dagger .

Armed with these, we now proceed to some simple calculations. As H is Hermitian,

$$\begin{aligned} H^\dagger &= e^{-V_N/2T_{cl}} H_{FP}^\dagger e^{V_N/2T_{cl}}, \\ (=H) &= e^{V_N/2T_{cl}} H_{FP} e^{-V_N/2T_{cl}}. \end{aligned} \quad (38)$$

Explicitly multiplying by $e^{V_N/2T_{cl}}$ on the left and by $e^{-V_N/2T_{cl}}$ on the right leads to

$$H_{FP}^\dagger = e^{V_N/T_{cl}} H_{FP} e^{-V_N/T_{cl}}. \quad (39)$$

We will now prove that the state $|+\rangle$ is a left eigenstate of the Fokker-Planck Hamiltonian with zero eigenvalue. Beginning with a simple extension of the definition of the ground state,

$$H_{FP}|G\rangle = 0 \rightarrow \langle G | H_{FP}^\dagger = 0. \quad (40)$$

As is evident from Eq. (39), this is equivalent to

$$\langle G | e^{V_N/T_{cl}} H_{FP} e^{-V_N/T_{cl}} = 0, \quad (41)$$

which [from Eqs. (34) and (36)] implies that

$$Z_N^{-1} \langle + | H_{FP} e^{-V_N/T_{cl}} = 0. \quad (42)$$

This illustrates that this uniform state is a left null eigenstate²⁶ for all Fokker-Planck Hamiltonians (i.e., $\langle + | H_{FP} = 0$).

We will now derive our new central result of Eq. (9). Towards this end, we write anew the classical correlation function of Eq. (8):

$$G_{\text{classical}}(t) = \langle \mathcal{O}_1(t) \mathcal{O}_2(0) \rangle. \quad (43)$$

By Bayes' theorem, the joint probability distribution, $P(\{\vec{x}\}, \{\vec{y}\}) = P(\{\vec{x}\} | \{\vec{y}\}) P(\{\vec{y}\})$, the probability of finding coordinates $\{\vec{x}\}$ at time t and coordinates $\{\vec{y}\}$ at time 0, is given by the product of the conditional probability of finding $\{\vec{x}\}$ at time t given $\{\vec{y}\}$ at time 0 with the probability of attaining $\{\vec{y}\}$ at time $t = 0$. For a lattice system with fields ϕ at different lattice sites (which we will briefly return to in Appendix E), the equality $P(\{\vec{x}\}, \{\vec{y}\}) = P(\{\vec{x}\} | \{\vec{y}\}) P(\{\vec{y}\})$ is to be replaced by $P[\{\phi(\vec{x}, t)\}, \{\phi(\vec{x}, 0)\}] = P[\{\phi(\vec{x}, t)\} | \{\phi(\vec{x}, 0)\}] P[\{\phi(\vec{x}, 0)\}]$. As discussed in Sec. III A, the ground state has a probability distribution given by a Boltzmann distribution $Z_N^{-1} e^{-\beta V_N(\{y\})}$

[see Eq. (34)]. The conditional probability $P(\{x\} | \{y\})$ can be expressed in terms of the matrix element of $\mathcal{T} e^{-\int_0^t H_{FP}(t') dt'}$ (where \mathcal{T} is the time-ordering operator) as this conditional P satisfies Eq. (19). With \mathcal{O}_1 depending on the coordinates $\{\vec{y}\}$ at time t and \mathcal{O}_2 on the coordinates $\{\vec{x}\}$ at time $t = 0$, all this implies the form of the expectation value of Eq. (43):

$$\begin{aligned} G_{\text{classical}}(t) &= \int d^{dN} x d^{dN} y \mathcal{O}_1 P(\{\vec{x}\}, \{\vec{y}\}) \mathcal{O}_2 \\ &= \int d^{dN} x d^{dN} y \mathcal{O}_1 P(\{\vec{x}\} | \{\vec{y}\}) \mathcal{O}_2 P(\{\vec{y}\}) \\ &= \int d^{dN} x d^{dN} y \mathcal{O}_1 \langle \{\vec{x}\} | \mathcal{T} e^{-\int_0^t H_{FP}(t') dt'} | \{\vec{y}\} \rangle \mathcal{O}_2 \\ &\quad \times \frac{e^{-\beta V_N(\{\vec{y}\})}}{Z_N}. \end{aligned} \quad (44)$$

It is important to reiterate and emphasize yet again that, in the last line above, we only assume that *the initial state* ($|\{\vec{y}\}\rangle$ at time $t = 0$) is in thermal equilibrium. *The system need not be in thermal equilibrium at positive times.* As stated earlier, this is the sole assumption made in this derivation for general time-dependent systems with dynamical V_N (and thus for time-dependent Fokker-Planck operators). A similar derivation would hold *mutatis mutandis* when the system is initially out of equilibrium and is in equilibrium in its final state.

Equation (36) asserts that $\int d^{dN} x \langle \{\vec{x}\} | = \langle + |$. Invoking this along with Eq. (34), we have that

$$G_{\text{classical}}(t) = \langle + | \mathcal{O}_1 \mathcal{T} e^{-\int_0^t H_{FP}(t') dt'} \mathcal{O}_2 | G \rangle. \quad (45)$$

As is evident from Eq. (42), inserting an exponentiation of H_{FP} to the right of the state $\langle + |$ leads to a multiplication by unity. Thus, Eq. (45) can be rewritten as

$$G_{\text{classical}}(t) = \langle + | \mathcal{T} e^{\int_0^t H_{FP}(t') dt'} \mathcal{O}_1 \mathcal{T} e^{-\int_0^t H_{FP}(t') dt'} \mathcal{O}_2 | G \rangle. \quad (46)$$

With the aid of Eq. (37), we can express this quantity in terms of the quantum Hamiltonian H instead of H_{FP} :

$$\begin{aligned} G_{\text{classical}}(t) &= \langle + | e^{-V_N/(2T_{cl})} \mathcal{T} e^{\int_0^t H(t') dt'} \mathcal{O}_1 \\ &\quad \times \mathcal{T} e^{-\int_0^t H(t') dt'} e^{V_N/(2T_{cl})} \mathcal{O}_2 | G \rangle. \end{aligned} \quad (47)$$

Rather explicitly multiplying and dividing by $\sqrt{Z_N}$,

$$\begin{aligned} G_{\text{classical}}(t) &= \langle + | \frac{e^{-V_N/(2T_{cl})}}{\sqrt{Z_N}} \mathcal{T} e^{\int_0^t H(t') dt'} \mathcal{O}_1 \mathcal{T} e^{-\int_0^t H(t') dt'} \\ &\quad \times \mathcal{O}_2 \sqrt{Z_N} e^{V_N/(2T_{cl})} | G \rangle. \end{aligned} \quad (48)$$

As discussed in Sec. III A 1 [in particular, Eq. (28)], the ground state of the quantum system is given by $|0\rangle = \sqrt{Z_N} e^{V_N/(2T_{cl})} |G\rangle$. Further invoking Eqs. (34) and (36), we can rewrite Eq. (48) as

$$G_{\text{classical}}(t) = \langle 0 | \mathcal{T} e^{\int_0^t H(t') dt'} \mathcal{O}_1 \mathcal{T} e^{-\int_0^t H(t') dt'} \mathcal{O}_2 | 0 \rangle. \quad (49)$$

Note that, in this equation, $|0\rangle$ is the ground state of the system defined by the quantum Hamiltonian H . Our results above are general. We will shortly use Eq. (49) in order to relate it to correlations in the quantum system. Under the exchange of t by (it) , the reader may recognize Eq. (49) as a correlation function in the quantum system. One very simple point which is worth emphasizing is that not only the ground state of Eq. (28) is

trivially normalized but, of course, any state formed by the evolution with the unitary time-ordered exponential $\mathcal{U}(t) = e^{-i \int_0^t H(t') dt'}$.

In the quantum arena, it is clear that for a system initially prepared in the ground state $|0\rangle$ and then evolved with some Hamiltonian $H(t)$, the corresponding correlation function is given by

$$G_{\text{Quantum}}(t) = \langle 0 | \mathcal{T} e^{i \int_0^t H(t') dt'} \mathcal{O}_1 \mathcal{T} e^{-i \int_0^t H(t') dt'} \mathcal{O}_2 | 0 \rangle. \quad (50)$$

By comparing Eq. (49) with (50), Eq. (9) immediately follows. The fundamental relation of Eq. (9) establishes the connection between the overdamped Langevin equation of a classical particle at finite temperature and the Schrödinger equation of the dual quantum Hamiltonian. We suspect that related to this result is the fluctuation-dissipation theorem that relates correlation functions with the expectation value of time-ordered products in equilibrium (see, for example, Ref. 20, Chap. 13).

A derivation similar to that above can be performed for a correlation function involving an arbitrary number of operators. In the classical arena, such a correlation function takes the form of

$$G_{\text{classical}} = \langle \mathcal{O}_1(t_1) \mathcal{O}_2(t_2) \dots \mathcal{O}_n(t_n) \rangle, \quad (51)$$

where \mathcal{O}_i are arbitrary operators and $t_1 < t_2 < \dots < t_n$. Similar to our earlier calculations, by Bayes' theorem, this correlation function is given by

$$\begin{aligned} & \int d^{dN} x_1 d^{dN} x_2 \dots d^{dN} x_n \mathcal{O}_n \\ & \times \langle \{\vec{x}_n\} | \mathcal{T} e^{-\int_{t_{n-1}}^{t_n} H_{\text{FP}}(t') dt'} | \{\vec{x}_{n-1}\} \rangle \mathcal{O}_{n-1} \\ & \times \dots \langle \{\vec{x}_2\} | \mathcal{T} e^{-\int_{t_1}^{t_2} H_{\text{FP}}(t') dt'} | \{\vec{x}_1\} \rangle \mathcal{O}_1 \frac{e^{-\beta V_N(\{\vec{x}_1\})}}{Z_N}. \end{aligned} \quad (52)$$

Invoking identity matrix insertions and integrations over a complete set of eigenstates as before, this reduces to

$$\begin{aligned} & \langle + | \mathcal{T} e^{-\int_{t_n}^{t_1} H_{\text{FP}}(t') dt'} \mathcal{O}_n \mathcal{T} e^{-\int_{t_{n-1}}^{t_n} H_{\text{FP}}(t') dt'} \mathcal{O}_{n-1} \\ & \times \dots \mathcal{T} e^{-\int_{t_1}^{t_2} H_{\text{FP}}(t') dt'} \mathcal{O}_1 | G \rangle. \end{aligned} \quad (53)$$

Transforming to the quantum Hamiltonian $H(t)$ and its respective ground state at time $t = 0$ yields

$$\begin{aligned} & \langle 0 | \mathcal{T} e^{-\int_{t_n}^{t_1} H(t') dt'} \mathcal{O}_n \mathcal{T} e^{-\int_{t_{n-1}}^{t_n} H(t') dt'} \mathcal{O}_{n-1} \\ & \times \dots \mathcal{T} e^{-\int_{t_1}^{t_2} H(t') dt'} \mathcal{O}_1 | 0 \rangle. \end{aligned} \quad (54)$$

The remainder of the derivation is similar to that in the two-time case. In order to transition from the classical to the quantum system, we replace, in all pertinent correlation functions, the times $\{t_a\}_{a=1}^n$ by $\{it_a\}_{a=1}^n$.

We next return to the two-time correlation function and discuss the quantum response function R_{Quantum} that monitors the change in the average value of \mathcal{O}_1 as a result of a perturbation \mathcal{O}_2 . We first review standard textbook³⁸ results concerning quantum linear response functions and then invoke our new result of Eq. (9) to obtain zero temperature quantum linear response functions given corresponding results on finite temperature classical duals. Towards this end, we first consider

the Hamiltonian

$$H_{\text{tot}} = H + H', \quad (55)$$

where H' is a small perturbation which can be expressed as $H' = -\lambda \mathcal{O}_2$. We next review the standard protocol for computing the lowest-order deviation

$$\delta \langle \mathcal{O}_1(t) \rangle = \langle \mathcal{O}_1(t) \rangle_\lambda - \langle \mathcal{O}_1(t) \rangle_0, \quad (56)$$

which we will evaluate within the ground state $|0\rangle$. This deviation is readily computed within the interaction picture where we evolve with the time-ordered exponential $T \exp(-iH't)$:

$$\begin{aligned} \langle \mathcal{O}_1(t) \rangle_\lambda & \approx \left\langle \left(1 - i \int^t dt' \lambda(t') \mathcal{O}_2(t') \right) \mathcal{O}_1(t) \right. \\ & \left. \times \left(1 + i \int^t dt' \lambda(t') \mathcal{O}_2(t') \right) \right\rangle. \end{aligned} \quad (57)$$

Collecting terms to lowest order,

$$\begin{aligned} \delta \langle \mathcal{O}_1(t) \rangle & \approx i \int^t dt' \lambda(t') \langle [\mathcal{O}_1(t), \mathcal{O}_2(t')] \rangle \\ & = i \int_0^\infty d\tau \lambda(t - \tau) \langle [\mathcal{O}_1(t), \mathcal{O}_2(0)] \rangle \\ & \equiv \int_{-\infty}^\infty d\tau \lambda(t - \tau) R_{\text{Quantum}}(\tau). \end{aligned} \quad (58)$$

As $\mathcal{O}_1(t) = \mathcal{T} e^{-i \int_0^t H(t') dt'} \mathcal{O}_1 \mathcal{T} e^{i \int_0^t H(t') dt'}$, from the last line of Eq. (58), the quantum response function

$$R_{\text{Quantum}}(t) = i \Theta(t) \langle 0 | [\mathcal{T} e^{i \int_0^t H(t') dt'} \mathcal{O}_1 \mathcal{T} e^{-i \int_0^t H(t') dt'}, \mathcal{O}_2] | 0 \rangle. \quad (59)$$

Comparing Eqs. (49) and (59), we derive Eq. (10) by further expanding it to get the imaginary part of the analytically continued classical correlation function

$$\begin{aligned} R_{\text{Quantum}}(t) & = i \Theta(t) [G_{\text{classical}}(it) - G_{\text{classical}}^*(it)] \\ & = -2\Theta(t) \text{Im} G_{\text{classical}}(it). \end{aligned} \quad (60)$$

C. Fields on a lattice

We conclude this section with a brief discussion of the duality for fields on lattice sites. If we replace Eq. (5) by

$$\gamma_i \frac{d\phi_i}{dt} = -\frac{\delta}{\delta\phi_i} V_N(\phi_1, \dots, \phi_N) + \eta_i(t) \quad (61)$$

to describe a classical lattice system with fields ϕ_i at the various lattice points i , then trivially replicating all of our calculations thus far with the exchange $\vec{x}_i \rightarrow \phi_i$ (including in all gradient or variational derivative operators), we will arrive at a corresponding quantum lattice system *mutatis mutandis*.

IV. HIGH-DIMENSIONAL QUANTUM GLASS MODELS DERIVED FROM CLASSICAL COUNTERPARTS

In the next sections, we will examine the consequences of Eq. (9) for disparate quantum systems. As outlined earlier, our basic three-prong approach will be rather simple: (1) We take a classical dissipative system whose dynamical behavior is known at finite temperatures [including, in particular, pertinent

temporal correlation functions of the form of Eq. (8)]. (2) We determine the corresponding dual quantum Hamiltonian using Eq. (7) or its explicit form for classical pair potentials which we detail below. (3) We next invoke Eq. (9) in order to determine the very same correlation function of Eq. (8), yet now at zero temperature for the dual quantum Hamiltonians.

In this section, we will detail a few (of the many known) classical glassy systems for which our results for the quantum duals will hold. The specific heavily investigated classical dissipative systems that we focus on all exhibit glassy dynamics. It is worth emphasizing that the results that we will obtain using our three-prong approach *do not rely on any special integrability of the quantum models*. Rather, by using the multitude of available information on the quantum glass system, we will be able to make exact statements on numerous quantum systems.

We consider what specifically occurs when the classical potential energy in Eq. (5) is the sum of pairwise interactions (as it typically is)

$$V_{\text{N}}(\{\vec{x}\}) = \frac{1}{2} \sum_{i \neq j} V_{ij}(\vec{x}_i - \vec{x}_j). \quad (62)$$

For such systems, the quantum many-body Hamiltonian of Eq. (7) explicitly contains an effective potential which is the sum of two- and three-body interactions:

$$\begin{aligned} \mathcal{V}_{\text{Quantum}}(\{\vec{x}\}) &= \sum_i \frac{1}{\gamma_i} \left[-\frac{1}{2} \nabla_i^2 V_{\text{N}} + \frac{1}{4T_{cl}} (\vec{\nabla}_i V_{\text{N}})^2 \right] \\ &= -\frac{1}{2} \sum_{i \neq j} \frac{1}{\gamma_i} \nabla_i^2 V_{ij} + \sum_{i,j \neq i; j' \neq i} \frac{\vec{\nabla}_i V_{ij} \cdot \vec{\nabla}_i V_{ij'}}{4T_{cl} \gamma_i}. \end{aligned} \quad (63)$$

For a given classical two-body potential in d dimensions which is both translationally and rotationally invariant, $V(\vec{x}) = V(|\vec{x}|)$, the resulting quantum potential energy is given by (as in Ref. 26 yet now trivially extended to general classical temperatures T_{cl})

$$\begin{aligned} \mathcal{V}_{\text{Quantum}}(\{\vec{x}\}) &= \frac{1}{2} \sum_{i \neq j} v_{\text{Quantum}}^{\text{pair}}(\vec{x}_i - \vec{x}_j) \\ &\quad + \sum_{i,j \neq i; j' \neq i} v_{\text{Quantum}}^{\text{3-body}}(\vec{x}_i - \vec{x}_j, \vec{x}_i - \vec{x}_{j'}); \\ v^{\text{pair}}(\vec{x}) &= -\nabla^2 V(\vec{x}) + \frac{1}{2T_{cl}} [\vec{\nabla} V(\vec{x})]^2 \\ &= -\frac{d-1}{r} V'(r) - V''(r) + \frac{1}{2T_{cl}} [V'(r)]^2; \\ v^{\text{3-body}}(x, x') &= \frac{1}{4T_{cl}} \vec{\nabla} V(x) \cdot \vec{\nabla} V(x') \\ &= \frac{1}{4T_{cl}} \frac{\vec{x}}{r} \cdot \frac{\vec{x}'}{r'} V'(r) V'(r'), \end{aligned} \quad (64)$$

with $r = |\vec{x}| = |\vec{x}_i - \vec{x}_j|$ and, in the three-body term, $r' = |\vec{x}'| = |\vec{x}_i - \vec{x}_{j'}|$. For short-range classical interactions $V(r)$, the three-body term can be appreciable only if the three points (i, j, j') in the second sum of Eq. (64) defining the distances r and r' all lie within the short distance of one another where the classical potential operates. Thus, statistically, the three-body

interactions are typically insignificant by comparison to, the far more dominant, pair interaction terms in Eq. (64).

As we explained in Sec. III A, whenever the classical potential V_{N} is invariant under the permutations of the coordinates of any pair of particles [as it explicitly is when it is the sum of symmetric pair interactions $V(|\vec{x}_i - \vec{x}_j|)$], then the resulting quantum many-body system is bosonic. In Appendix D (and, to a lesser degree in Appendix E), we elaborate how our results can, as a matter of principle, be explicitly extended to specific fermionic systems (which are of great pertinence in our goal of illustrating the feasibility of the behaviors that we study in this work for electronic systems).

Although our results in the sections that follow are very general, it is nevertheless useful to have concrete models in mind. We next detail some typical model systems that we will refer to. These systems include both off-lattice liquid and lattice systems. The liquids that we list exhibit fluid behavior at high classical temperatures and glasslike features at high densities and/or low temperatures. *Within the highly viscous low-temperature regime, the classical fluids that we list below become overdamped and may be modeled by Eq. (5).*

Liquid models. (a) As a first example, we list a system of three-dimensional spheres (s). The classical potential associated with this system is given by $V_s(r) = V_0 \exp\{-\lambda[(r/\sigma)^2 - 1]\}$. This model has been extensively studied.²⁶ In this system, the potential V_s has a clear finite range (set by the diameter of the spheres σ). Following our earlier discussion, the magnitude of the three-body term in Eq. (64) will be negligible by comparison to that of the pair interactions. The corresponding pair term set by Eq. (64) is

$$v^{\text{pair}}(r) = \frac{2\lambda d - 4\lambda^2 r^2}{\sigma^2} V_s(r) + \frac{2\lambda^2 r^2}{T_{cl} \sigma^4} [V_s(r)]^2. \quad (65)$$

In the limit $\lambda \rightarrow \infty$, the classical system corresponds to that of hard spheres where σ is the diameter of the hard sphere and the quantum potential of Eq. (65) similarly exhibits a dominant hard-sphere repulsion (augmented by an attractive potential at the sphere boundaries that is of range $1/\lambda$). In the sections that follow, we will refer to the finite temperature ($T_{cl} > 0$) behavior of this system (and the other models below). In the hard-sphere ($\lambda \rightarrow \infty$) limit, this system becomes temperature independent. (b) A classical bidisperse repulsive system given by the pair potential³⁹

$$V_{ab}(r) = \epsilon \left(\frac{\sigma_{ab}}{r} \right)^{12} \quad (66)$$

between two particles (a, b) of two possible types [$(a, b) \in 1, 2$] with $\sigma_{ab} = (\sigma_a + \sigma_b)/2$ and $\sigma_2/\sigma_1 = 1.2$. The corresponding quantum potential is given by Eq. (64). It is this full potential that leads to the exact same dynamical correlation functions for the quantum system following Eq. (9). Similar to (a), for pair distances larger than σ_{ab} , the three-body term in the quantum Hamiltonian of Eq. (64) is far smaller than the pair interaction term. Thus, at low temperatures $T_{cl} \ll \epsilon$, in any number of dimensions d , this classical system has a quantum dual given by a pair potential

$$v_{ab}^{\text{pair}}(r) \simeq \frac{72\epsilon\sigma_{ab}^{24}}{T_{cl}r^{26}}. \quad (67)$$

(c) A classical bidisperse Lennard-Jones mixture. Similar to (b), this is a model of two species: 1,2. Unlike (b), however, each pair of atoms (a,b) interact via a Lennard-Jones-type interaction

$$V_{ab}(r) = \epsilon_{ab} \left[\left(\frac{\sigma_{ab}}{r} \right)^{12} - \left(\frac{\sigma_{ab}}{r} \right)^6 \right]. \quad (68)$$

This augments the repulsive only potential of (b) by an additional longer-range attractive interaction. In the standard Kob-Andersen mixtures⁴⁰ that we will refer to, $\epsilon_{12}/\epsilon_{11} = 1.5, \epsilon_{22}/\epsilon_{11} = 0.5$ with similar lengths σ_{ab} as in (b). The zero temperature quantum dual of a low-temperature classical system ($T_{cl} \ll \epsilon_{11}$) is

$$v_{ab}^{\text{pair}}(r) \simeq \frac{18\epsilon_{ab}^2 \sigma_{ab}^{12}}{T_{cl} r^{14}} \left[1 - 4 \left\{ \left(\frac{\sigma_{ab}}{r} \right)^6 - \left(\frac{\sigma_{ab}}{r} \right)^{12} \right\} \right]. \quad (69)$$

Lattice models. (d) The $N3$ and $N2$ lattice models^{41,42} (which share some similarity with earlier lattice glass models⁴³). In the square lattice $N3$ model, particles are endowed with hard-core repulsive interactions that extend up to a distance of three steps on the lattice. Similarly, in the cubic lattice $N2$ model particles can not be nearest neighbors nor next-nearest neighbors (i.e., the repulsive hard-core interactions extend up to a distance of two steps on the lattice). In Secs. VI and VII, we will further motivate and discuss quantum lattice systems.

At their core, the results that we discuss next are not limited to the examples (a)–(d) above nor to simple classical pair interactions. Given any classical system whose evolution is given by Eqs. (5) and (19), the corresponding dual quantum system is provided by Eqs. (7) and (21). This can, e.g., include models of classical dislocation motion and turbulence in liquids.

V. GLASSY DYNAMICS IN OFF-LATTICE QUANTUM FLUIDS

Armed with all of the background and results described in earlier sections, we now proceed to derive general physical results in quantum systems. Our aim is to show that as a matter of principle, zero-point quantum fluctuations can lead to very rich glass-type behaviors in numerous many-body systems which mirror those that appear in dissipative classical systems at finite temperatures. As we alluded to in the Introduction, classical liquids may become quenched into a glassy state when they are rapidly cooled (“supercooled”) below structural freezing temperatures and fall out of thermal equilibrium. Invoking Eq. (9), this will suggest that in the zero temperature quantum duals, a corresponding phenomenon will occur: quantum fluids may veer towards a glassy state as parameters are rapidly changed in time. As we emphasized earlier, our derivation of Sec. III B allowed (as is physically crucial) for time-dependent Hamiltonians which emulate rapid changes in the classical temperature or any other parameters in the interaction and for classical final (or initial) states which are out of equilibrium. Its sole assumption was that the average over the noise at any instant of time was still afforded by Eq. (6) with T_{cl} the corresponding classical temperature at that time.

We focus on measurable quantities that may be ascertained from response functions.

Response functions in classical glass-forming liquids which become progressively more viscous and become frozen into a glass as their temperature is rapidly lowered (as well as response functions in various electronic systems) suggest the presence of a distribution of local relaxation times that lead to, e.g., the canonical Cole-Cole or Cole-Davidson^{44,45} and similar forms as we briefly elaborate on. In various guises, all of the models discussed in Sec. IV exhibit glasslike features including notably the distribution of relaxation times which we discuss now.

The response of a single attenuated mode to an initial impulse at time $t = 0$ scales as $g_{\text{single}} \sim \exp(-t/\tau)$ with τ the relaxation time; the Fourier transform of this response is $g_{\text{single}}(\omega) = g_0/(1 - i\omega\tau)$. In systems with a *distribution* $f(\tau')$ of relaxation events, the response functions are given by $\int d\tau' f(\tau') \exp(-t/\tau')$. Empirically, in dissipative plastic or viscoelastic systems, relaxations scale as $\exp[-(t/\tau)^c]$ with a power $0 < c < 1$ that leads to a “stretching” of the response function. This stretched exponential and other similar forms, such as the Cole-Cole (CC) and Davidson-Cole (DC) functions, quintessentially capture the distribution of relaxation times.^{44,45} With $g(\omega) = g_0 G(\omega)$, where g_0 is a constant, the CC and CD forms correspond to different choices of G :

$$G_{\text{CC}}(\omega) = \frac{1}{[1 - (i\omega\tau)^{\bar{\mu}}]}, \quad G_{\text{DC}}(\omega) = \frac{1}{[1 - i\omega\tau]^{\bar{\nu}}}. \quad (70)$$

The parameters $\bar{\mu}$ and $\bar{\nu}$ qualitatively emulate the real-time stretching exponent c . This distribution of relaxation times might be associated with different local dynamics (dynamical heterogeneities) to which we will turn to shortly in Sec. V A. As liquids are supercooled, their characteristic relaxation times and viscosity may increase dramatically. There are several time scales that govern the dynamics of supercooled liquids. The so-called “ α (or primary) relaxation” is associated with cooperative motion and leads to a pronounced rise of the viscosity (especially so in the “fragile” glass formers). Empirically, in real classical supercooled liquids at a temperature T_{cl} , the α relaxation times follow the Vogel-Fulcher-Tammann form⁴⁶

$$\tau(T_{cl}) = \begin{cases} \tau_0 e^{D T_0 / (T_{cl} - T_0)} & \text{for } T > T_0, \\ \infty & \text{for } T \leq T_0. \end{cases} \quad (71)$$

Here, T_0 is the temperature of the classical system at which the relaxation times [if Eq. (71) is precise] will truly diverge and D is a dimensionless constant. Mode coupling theory⁴⁷ and numerous other theories might similarly capture aspects of the increase in the α relaxation time. In a low-temperature liquid, augmenting the long-time α relaxations to equilibrium, there are so-called “ β (or secondary) relaxations”⁴⁸ which further manifest in local relaxation processes. The β relaxation times scale with temperature in an Arrhenius-type fashion:

$$\tau_{\text{secondary}} \sim e^{\Delta/T_{cl}} \quad (72)$$

with Δ a temperature-independent constant. Recent work suggests intriguing relations between α and β relaxations.⁴⁹ By virtue of Eq. (9), the finite temperature classical α (and β) relaxations and their associated stretched exponential-type relaxations all have zero temperature quantum duals. In

the quantum arena, as discussed in Sec. III, the classical temperature T_{cl} is replaced by the effective mass $m = \gamma/(2T_{cl})$ and parametrical changes in the many-body potential $\mathcal{V}_{\text{Quantum}}(\{\vec{x}\})$.

The classical hard-sphere limits of models (a) and (d) of Sec. IV are athermal; in these models, a glass-type state may only be arrived at by varying the system density. By contrast, in models (b) and (c) [as well as away from the hard-sphere limit of model (a)] lowering the temperature may induce a transition into a glass. By a trivial application of our result of Eq. (10), all of these finite temperature classical forms have the same quantum zero temperature counterparts. Thus, *the relaxation times in the quantum dual models scale in precisely the same way as they do in the classical glass-forming systems* [including Eq. (71) for duals to classical glass formers]. Slower dynamics also appears as the system density increases. Several works, e.g., Ref. 50, suggest that relaxation times are a function of a composite quantity involving both density and temperature. It should be noted that all of our derivations start from Eq. (5). When examining the quantum dual to empirical forms describing classical liquids, the bare viscosity [or associated bare relaxation time τ_0 in Eq. (71)] of the ambient liquid appearing in these equations of motion may, in principle, be allowed to change as the temperature (and density) are varied. These may appear in addition to changes in T_{cl} and V_N (capturing, e.g., changes in the density). In classical simulated liquids, the bare viscosity may be kept constant.

A. Quantum dynamical heterogeneities and relations for four-point correlators

We now focus on an intriguing aspect of classical glasses which by virtue of the relation of Eqs. (9) and (10) (as alluded to in Ref. 15) leads to the appearance of new dynamical correlations in quantum systems. Disorder-free models for classical glass formers (including various simulated quenched systems such as those endowed with various classical potentials V_N discussed in Sec. IV that do not permit simple crystalline orders) are known to exhibit “dynamical heterogeneities” (DH), i.e., a nonuniform distribution of local velocities⁵¹ with the location of the more rapidly moving particles changing with time. By invoking Eqs. (9) and (10), we see that *quantum dynamical heterogeneities*¹⁵ (QDH) appear in their corresponding zero temperature quantum counterparts. That is, in disorder-free quantum systems derived [via Eq. (7)] from the corresponding classical systems, zero point dynamics is spatially nonuniform.

The presence of DH is empirically seen by numerous probes⁵¹ in real glass formers as well as model systems (including all of the systems in Sec. IV). As we alluded to earlier, one often used metric is that of the four-point correlations of Eq. (3) in various guises. These correlation functions are of the form of Eq. (8) with $\mathcal{O}(t)$ denoting the overlap between fields ϕ when these are separated in time:

$$\mathcal{O}_{\vec{q}}(t) = \phi_{\vec{q}}(t)\phi_{-\vec{q}}(0) - \langle \phi_{\vec{q}}(t) \rangle \langle \phi_{-\vec{q}}(0) \rangle, \quad (73)$$

with \vec{q} any wave vector. When Eq. (73) is substituted into Eqs. (8) and (9), the four-point correlator can be computed. Classically, the Fourier space correlation functions [denoted $S_4^{\text{classical}}(\vec{q}, t)$ below] typically have an Ornstein-Zernike-type

similar to that in critical phenomena⁵² or similar generalized (for a non-vanishing “anomalous exponent” η) forms that incorporate time dependence., e.g.,⁵³

$$S_4^{\text{classical}}(\vec{q}, t) = \frac{\chi_4(t)}{1 + (q\xi_4(t))^{2-\eta}}, \quad (74)$$

with the length scale $\xi_4(t)$ representing the size of the typical dynamical heterogeneity, when the system is examined at two times separated by an interval t . The four-point susceptibility $\chi_4(t)$ is simply set by $\int d^d x G_4(\vec{x}, t)$ [see Eq. (4)]. The key feature of Eq. (74) is that all of the q dependence has been relegated to a Lorentzian ($\eta = 0$) or similar ($\eta \neq 0$) form while χ_4 and ξ_4 are otherwise general time-dependent functions. We may next invoke Eqs. (9) and (10) to generate the quantum counterpart of Eq. (74) (or of any other related form) and Fourier transform to real space to obtain, in the notation of Eq. (3), the spatial quantum correlation function $G_4^{\text{Quantum}}(\vec{x} - \vec{y}, t)$ associated with the potential $\mathcal{V}_{\text{Quantum}}$ of Eq. (64). The Fourier integral will be dominated by momentum-space poles at $q = \pm i\xi_4^{-1}$. It is clear that in employing the transformation of Eqs. (9) and (10), $G_4^{\text{Quantum}}(\vec{x} - \vec{y}, t)$ will exhibit exponential decay with the very same correlation length ξ_4 that is present in the classical system. This affords a direct proof of the dynamical length scale ξ_4 in *all zero temperature quantum counterparts* [given by Eq. (7)] to any dissipative classical system that is known to exhibit these (and there are numerous known classical systems that exhibit dynamical heterogeneities⁵¹).

B. Rapidly increasing time scale with concomitant slowly increasing length scale in quantum glasses

There is a proof that a growing static length scale must accompany the diverging relaxation time of glass transitions.¹⁰ Some evidence has indeed been found for growing correlation lengths (static and those describing dynamic inhomogeneities).^{54–57} As we noted earlier in this work, correlation lengths were studied via “point-to-set” correlations^{11,58} and pattern repetition size.⁵⁹ Other current common methods of characterizing structures include (a) Voronoi polyhedra,^{60–62} (b) Honeycutt-Andersen indices,⁶³ and (c) bond orientation;⁶⁴ all centering on an atom or a given link. More recent approaches include graph theoretical tools and various types of network analysis.^{65,66} Notwithstanding current progress, it is fair to say that currently most “natural” textbook-type length scales do not increase as dramatically as the relaxation time does when a liquid is supercooled and becomes a glass.

It is worthwhile to highlight that one of the most pertinent naturally increasing length scales is that associated with the typical size of the dynamical heterogeneity [i.e., ξ_4 of Eq. (74)]. Similar to other measures, this typical length scale does not increase as rapidly as the characteristic relaxation time does as the glass transition is approached. Recent work for a three-dimensional bidisperse repulsive glass⁶⁷ of Eq. (66) suggests that

$$\tau \sim \exp(k\xi_4^\theta), \quad (75)$$

with $\theta \simeq 1.3$ and k a constant. An alternate assumed algebraic form $\tau \sim \xi_4^z$ leads to a large dynamical exponent $z \simeq 10.8$.

In these cases, the dynamics changes dramatically with little notable change in the spatial correlation length.

C. Quantum critical jamming

The mapping between dissipative classical and quantum systems raises the specter of a new quantum critical point associated with jamming.¹⁵ Our discussion following employs the exact mapping of Eq. (9) to derive exact results on quantum jammed systems given the wealth of information on their classical counterparts.

The classical jamming transition^{68–79} of hard spheres [such as those of models (a) in Sec. IV] from a jammed system at high density to an unjammed one with spatially heterogeneous motion at lower densities is a continuous transition with known critical exponents, both static^{72,73} and dynamic.⁷⁹ The transition into the classical jammed phase may be brought about by a reduction in temperature, increase in particle density, and the application of stress. In most classical solids, the ratio of the shear to bulk modulus is a number of order unity (e.g., $\frac{1}{3}$ in many conventional three-dimensional solids). However, at the jamming threshold, this ratio tends to zero. Thus, jammed systems may be very susceptible to shear stresses. This softness is one of the peculiar features that sets jammed systems apart from conventional solids.⁶⁹ As seen by our mapping from classical to quantum systems, the classical jamming transition has a quantum analog with similar dynamics. Replicating the mapping of the previous section [and, in particular, Eq. (10) therein], we may derive an analog quantum system harboring a zero temperature transition with similar critical exponents. The classical zero temperature critical point (“point J ”)^{68,70} may rear its head anew in the form of *quantum critical jamming* (at a new critical point: “quantum point J ”) in bosonic systems. A schematic of the phase diagram of the associated quantum system is depicted in Fig. 1.

We may ascertain dynamical exponents from those reported for the classical jamming system.⁷⁹ The classical low-temperature system ($T_{cl} \rightarrow 0$) maps, according to Eq. (7), onto a zero temperature quantum system in its large-mass limit. Bosons of infinite mass are not trivial due their statistics. Specifically, for a classical system of monodisperse soft spheres with a repulsive force that is linear in the amount of compression, it was found that the correlation length ξ and relaxation time τ scale⁷⁹ as

$$\xi \sim (\rho_J - \rho)^{-0.7}, \quad \tau \sim (\rho_J - \rho)^{-3.3}. \quad (76)$$

In Eq. (76), ρ denotes the density with ρ_J being the critical density at the jamming transition marked by point J . Equation (76) describes how the spatial and time scales diverge as the density is increased and approaches (from below) the density at the jamming transition. The correlation length in the jammed systems is set by the scale at which the number of surface zero modes is balanced by bulk effects. Taken together, these imply that, on approaching the transition, the relaxation time increases much more rapidly than the correlation length $\tau \sim \xi_4^z$ with a large effective dynamical exponent $z \simeq 4.6$. By use of Eq. (10), the same behavior is to be expected for the quantum system governed by the corresponding quantum

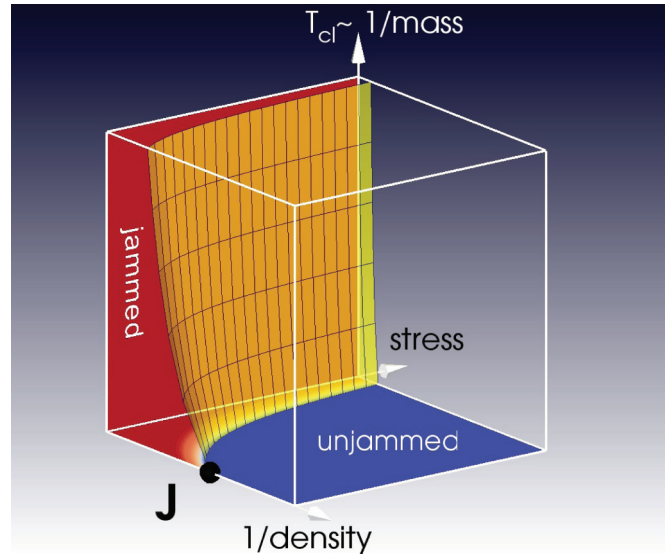


FIG. 1. (Color online) The phase diagram of the zero temperature quantum jamming transition with line of J points. The phase boundaries and axes were formed by employing the phase diagram of the classical system (Ref. 69) and examining the duality between the classical and quantum systems, i.e., comparing the parameters in the quantum system of Eq. (7) with the classical system defined by Eqs. (5) and (6).

potential $\mathcal{V}_{\text{Quantum}}$. The classical (and thus quantum) jamming exponents are the same in two and three dimensions.

It may be remarked that a similar dynamical exponent was found for a Bose glass model suggested to describe vortex lines in high-temperature superconductors.⁸⁰ In physical terms, for charged bosons, the jamming transition constitutes a transition from a metallic system (when the system is unjammed and behaves as a fluid) to a jammed state (an insulator). We note earlier work rationalizing metal to insulator transitions in terms of electron pinning.⁸¹ In the bosonic jamming that we describe above, no pinning is present and the transition is driven by particle interactions.

For completeness, we make one further remark concerning the physics of the jamming transition and its relation to the glass transitions that we discussed hitherto. As found in Refs. 82 and 83, ρ_J is an important density as it marks a change in the properties of the glass phase. That is, the conventional jamming transition does not correspond to a transition into a glass. Rather, point J and its finite temperature extension lies deep within a glassy phase that already onsets at a far lower density. The jamming transition at point J is associated with changes in the mechanical/structural properties of the glass phase. It is this transition that we depict in Fig. 1.

As in earlier sections, we see that time scales increase far more precipitously than spatial correlation lengths.

One of the hallmarks of classical jammed systems is that the spectral density of vibrational excitations $D(\omega)$ is constant at the jamming threshold.^{73,84} [In conventional Debye solids, $D(\omega) \sim \omega^2$.] This near constant value of $D(\omega)$ in jammed systems is independent of potential, dimension, and size of the system. Away from the jamming threshold, $D(\omega)$ exhibits a plateau down to a frequency ω^* . Below ω^* , the system

behaves similar to a Debye solid. This crossover frequency ω^* veers to zero on approaching the transition. The number of low-energy modes is set by the absence of constraints and Maxwell counting arguments. This constant density of states implies an enormous increase in the low-frequency excitations. These excitations can be probed by examining the trajectory of a single particle and Fourier transforming its motion. The corresponding modes are quasilocalized (or resonant) at low frequency below ω^* . Above ω^* , these modes are extended but still do not look at all like plane waves.⁶⁹

We now turn to the quantum systems derived by the mapping of Eq. (7). The results concerning the density of the modes in classical systems hold unchanged for their dual quantum counterparts. This is so as the dynamical matrix D is formed by the second derivatives of the potential V_N relative to the displacements. Thus, the same statement about mode density of states that appear in classical jammed systems holds verbatim in the classical potential V_N which we use to construct the quantum many-body potential $\mathcal{V}_{\text{Quantum}}(\{\vec{x}\})$ from Eq. (7). It follows that any appearance of zero-energy (bulk or surface) modes in the classical system will identically hold also in the quantum system.

VI. BOSONIC LATTICE SYSTEMS

Thus far, we largely focused on continuum viscous classical systems which, as we have seen, mapped onto continuum bosonic systems. We briefly remark here on classical lattice systems which similarly exhibit dynamical heterogeneities and a jamming-type transition. (In Sec. III C, we further briefly expanded on the extension of our derivation for lattice systems.) References 41 and 42 studied, respectively, the 2DN3 and 3DN2 models on the square and cubic lattice models in $d = 2$ and 3 dimensions. We provided details for these lattice models in the discussion of models of class (d) in Sec. IV. Similar to the continuum systems that we largely focused on until now, these models may be regarded as those of classical hard-core spheres. These finite-range hard-core interactions on the lattice thwart crystallization and lead to an amorphous jammed phase at high density. Following the mapping reviewed in Sec. III, the quantum Bose counterpart of such systems is that of dominant hard-sphere interactions augmented by contact sticky interactions. In the classical systems, simulation starts^{41,42} with an infinitely fast quenching wherein particles are added whenever possible and diffuse otherwise; this process is halted when the desired density is reached. A clear increase was noted in the length scales that characterize the dynamical heterogeneity.^{41,42} The continuum jamming transition discussed earlier may have a lattice counterpart for Cooper pairs as we now elaborate on. The jammed phase is that of an insulating (or Mott) phase of hard-core bosons forming a Hubbard-type system. Specifically, a natural quantum counterpart to the N3 (N2) model is given by an extended Bose-Hubbard-type^{85,86} model with infinite hard-core repulsions

$$H = -t \sum_{(ij)} (b_i^\dagger b_j + \text{H.c.}) + U \sum_i n_i (n_i - 1) + \sum_{ij} V_{ij} n_i n_j, \quad (77)$$

where $V_{ij} \rightarrow \infty$ for lattice sites i and j which are fewer than four (or three) steps apart and the onsite Hubbard repulsion U is divergent ($U \rightarrow \infty$) as well. The Hubbard term leads to a penalty only when there is a double or higher occupancy. Based on our considerations thus far, we expect to obtain the quantum bosonic counterpart to the classical jamming transitions found in the classical 2DN3 and 3DN2 models. This bosonic system may have all of the characteristics of the classical jammed system including dynamical heterogeneities and a large dynamical exponent z . For completeness, we briefly comment on the difference between the lattice system of Eq. (77) and the ‘‘Bose glass’’ first introduced in Ref. 85. The Bose glass appears in the bare (i.e., that with $V_{ij} = 0$) disordered rendition of Eq. (77) with the general Bose-Hubbard Hamiltonian (with general finite repulsion U) being further augmented by a local chemical potential term $-\sum_i \mu_i n_i$ wherein μ_i is a spatially nonuniform random quantity. By contrast, the lattice Hamiltonian of Eq. (77) as well as the continuum models that we discussed in earlier sections are free of disorder. The amorphous characteristics that these clean systems may exhibit are borne out of ‘‘self-generated’’ randomness,⁸⁷ not randomness that is present in the parameters defining the system.

VII. ELECTRONIC SYSTEMS WITH PAIRING INTERACTIONS

Up to now, building on and extending the mapping between classical dissipative systems and zero temperature bosonic theories, we focused on hard-core bosons. We now turn to the ground states of Fermi systems. In particular, in this section, we will consider standard electronic systems with pairing interactions

$$H = \sum_{\vec{k}, \sigma} \epsilon_{\vec{k}} c_{\vec{k}\sigma}^\dagger c_{\vec{k}\sigma} + \sum_{\vec{k}, \vec{l}} V_{\vec{k}, \vec{l}} c_{\vec{k}\uparrow}^\dagger c_{-\vec{k}\downarrow}^\dagger c_{-\vec{l}\downarrow} c_{\vec{l}\uparrow}, \quad (78)$$

where $\sigma = \uparrow, \downarrow$ is the spin-polarization index and V_{kl} is the interaction strength between the Cooper pairs $|\vec{k} \uparrow; -\vec{k} \downarrow\rangle$ and $|\vec{l} \downarrow; -\vec{l} \uparrow\rangle$. As is well known (and is readily verified), the Fermi bilinears

$$\begin{aligned} \bar{b}_{\vec{k}}^\dagger &= c_{\vec{k}\uparrow}^\dagger c_{-\vec{k}\downarrow}^\dagger, \\ \bar{b}_{\vec{k}} &= c_{-\vec{k}\downarrow} c_{\vec{k}\uparrow}, \end{aligned} \quad (79)$$

corresponding to the creation/annihilation of Cooper pairs satisfy hard-core Bose algebra. We next consider what occurs if, within the ground state and pertinent excited states generated by the (quenched or other) system time evolution, the occupancies of the single-particle states are correlated inasmuch as the electronic states on which the standard pairing Hamiltonian of Eq. (78) operates can only be created by applications of Cooper-pair creation operators on the vacuum [i.e., if the ground and relevant time evolved states are constrained to be invariant under the combined operations of parity ($\vec{k} \rightarrow -\vec{k}$) and time reversal ($\sigma \rightarrow -\sigma$)]. When the ground state is strictly invariant under the combined effect of these symmetries, we may express the Hamiltonian of Eq. (78)

as a bilinear in the hard-core Bose operators

$$H = \sum_{\vec{k}, \vec{l}} (2\epsilon_{\vec{k}} \delta_{\vec{k}, \vec{l}} + V_{\vec{k}, \vec{l}}) \bar{b}_{\vec{k}}^{\dagger} \bar{b}_{\vec{l}}. \quad (80)$$

The hard-core (Fourier space) Bose algebra of the creation and annihilation operators [as, in particular, manifest in the relation $(\bar{b}_{\vec{k}}^{\dagger})^2 = 0$ mandating that no more than one boson can occupy any given (Fourier space) site] is identical to that of raising and lowering operators in the spin $S = \frac{1}{2}$ system. Thus, a simple extension of the standard real-space Matsubara-Matsuda transformation⁸⁸ is given by

$$\bar{b}_{\vec{k}}^{\dagger} \rightarrow S_{\vec{k}}^{+}, \quad \bar{b}_{\vec{k}} \rightarrow S_{\vec{k}}^{-}. \quad (81)$$

Substituting Eq. (81) into Eq. (80), we arrive at an XY model. In situations in which the band dispersion $\epsilon_{\vec{k}}$ is nearly flat (and may be omitted for fixed particle number), in determining the ground state(s), we must only find the pairing V that affects pair hopping. Similar considerations apply in real space when Cooper pairs are short ranged and may be replaced by real-space hard-core bosons. In such cases, whenever the system is dominated by hard-core contact interactions between the bosonic Cooper pairs we see, replicating our analysis thus far, at zero temperature, that the system may undergo a jamming-type transition between an itinerant and jammed phase at sufficiently high densities or pressure. In this case, it displays rapidly increasing relaxation times concomitant with spatial correlations that do not increase as dramatically as the relaxation times do on approaching this transition.

VIII. POSSIBLE IMPLICATIONS FOR EXPERIMENTAL DATA

We now, very briefly, turn to a discussion of possible data analysis of experiments. One of the main messages of our work is that classical physics associated with overdamped classical systems can rear its head in the quantum arena. Correspondingly, data analysis which has led to much insight in the study of classical glasses and other damped systems may be performed anew for quantum systems. A principal correlation function which we focused on in this work has been that of the four-point correlation function of Eq. (3). This correlation function need not be directly measured in real time. For instance, scanning tunneling spectroscopy (STS) data taken at different positions and bias voltages may provide a valuable conduit towards the evaluation of the four-point correlator when it is expressed as an integral over frequencies (or associated bias voltages). Rather trivially with $\phi(\vec{x}, V)$ denoting the local density of states at location x for a bias voltage V , and e^* the electronic charge, the corresponding four-point correlation function is given by

$$\begin{aligned} G_4(\vec{x} - \vec{y}, t) = & \int dV_1 dV_2 dV_3 dV_4 \langle \delta\phi(\vec{x}, V_1) \delta\phi(\vec{x}, V_2) \\ & \times \delta\phi(\vec{y}, V_3) \delta\phi(\vec{y}, V_4) \rangle e^{ie^*t(V_1+V_3)} \\ & - C(\vec{x}, t) C(\vec{y}, t), \end{aligned} \quad (82)$$

with the two-point autocorrelation function

$$C(\vec{x}, t) = \int dV \langle \delta\phi(\vec{x}, V) \delta\phi(\vec{x}, 0) \rangle e^{ie^*tV}. \quad (83)$$

As seen from our discussion in Sec. V A concerning the Fourier-transformed four-point correlation function $S_4^{\text{classical}}(\vec{q}, t)$ in Eq. (74), quantum dynamical heterogeneities may be manifest in this correlation function.

IX. CONCLUSIONS

A central result of this work is the exact temporal correspondence of Eq. (10) that spans both equilibrium and nonequilibrium dynamics in general time-dependent systems (so long as either the initial or the final state of the classical system is that of thermal equilibrium). This equality relates (i) the autocorrelation function of Eq. (8), for *any quantity* \mathcal{O} when evaluated for the classical dissipative system of Eq. (5) with a many-body potential energy V_N , to (ii) the autocorrelation function of the very same corresponding quantum operator $\hat{\mathcal{O}}$ in a dual bosonic system governed by the Hamiltonian of Eq. (7). When fused with known results for dissipative classical systems, this extremely general equality immediately leads to numerous nontrivial effects which we introduced and readily proved as a matter of principle. These include the following:

(1) *Quantum dynamical heterogeneities* (QDH). We illustrated that similar to classical systems even in the absence of disorder, bosonic systems can, at zero temperature, exhibit spatially nonuniform zero-point motion. Of course, in translationally invariant systems, the average (time-averaged) dynamics is uniform. However, at any given time, there are particles that move more rapidly than others. We suggested how experimental data may be analyzed to search for quantum dynamical heterogeneities in electronic systems.

(2) The length scale characterizing the zero temperature QDH, the four-point correlation length ξ_4 (a trivial analog of its classical counterpart) may increase as the dynamics of the clean Bose system becomes progressively sluggish. However, albeit its rise, this length scale may increase much more slowly than the relaxation time. The far more rapid increase of the relaxation time as compared to readily measured length scales is a hallmark of many electronic systems. Cast in terms of quantum critical scaling (if and when it might be realized), the effective dynamical exponent z capturing the relation between correlation lengths and times is very large ($z \gg 1$). Other relations such as those of Eq. (75) may hold once they are established for viscous classical systems.

(3) The dramatic increase of primary relaxation times (which are far larger than the increase in conventional static length scales) with classical temperature as given by Eq. (71) [as well as the secondary relaxations of Eq. (72)] have direct zero temperature quantum analogs wherein changes in the classical temperature are replaced by a scaling of effective mass of particles and form of the many-body potential $\mathcal{V}_{\text{Quantum}}(\{\vec{x}\})$.

(4) Classical stretched exponential relaxations of the form of Eq. (11) have quantum analogs in the form of Eq. (12). In the quantum arena, there are sinusoidal modulations that multiply stretched exponential-type relaxations.

(5) Similar to classical systems, quantum systems may jam at high densities or pressure notwithstanding zero-point motion. The character of the jamming transition in zero temperature quantum systems is identical to that of their corresponding classical finite temperature counterparts. As

the classical systems exhibit a critical point at the jamming transition (at “point J ”), so do their bosonic counterparts. As a result, we established the existence of a quantum critical point associated with a *quantum critical jamming* of a hard-core Bose system. As in the other systems that we discussed, the characteristic relaxation time diverges more precipitously than the correlation length on approaching the transition (“quantum point J ”) with a large effective dynamical exponent $z \simeq 4.6$.

(6) The continuum theories that we predominantly focused on may have a broad applicability as continuum theories describe the same physics as their lattice renditions do in the vicinity of critical points. In Sec. VI, we discussed specific possible lattice renditions.

(7) The results that we derived for zero temperature bosonic theories suggest similar features in electronic systems. In some cases, as discussed in Sec. VII, finding the ground states of interacting electronic systems can be cast in terms of a corresponding zero temperature hard-core Bose problem.

(8) The general mapping of Eq. (81) between hard-core bosons to $S = \frac{1}{2}$ spin systems [in either momentum (\vec{k}) or real (\vec{r}) space] along with the complementary relation for the z component of the spin

$$[\bar{b}_k^\dagger \bar{b}_k - 1/2] \rightarrow S_k^z \quad (84)$$

in the same space allows us to derive similar results for certain spin $S = \frac{1}{2}$ systems. Spin models may exhibit transitions from spin-liquid-type phases to disorder-free glassy systems. In these systems, dynamical heterogeneities concomitant with a notable increase in relaxation-time scales may arise.

Thus, with the aid of the viscous classical many-body quantum correspondence of Eq. (10), we trivially established all of these results without the need to perform various standard and far more laborious computations for quantum systems.

Other possible extensions of our results include the relation between localization (or caging) in classical systems and their corresponding quantum counterparts. We may similarly examine disordered systems; for a random classical potential V_N , the corresponding quantum potential $\mathcal{V}_{\text{Quantum}}$ is also random. Although our focus has been on supercooled systems, Eq. (10) implies that also standard (nonglassy or spin-glassy) classical transitions have corresponding zero temperature quantum analogs.

As we discussed in detail [see Eq. (28)], if we are given a known quantum ground state, we may find the corresponding effective classical potential. With the aid of calculations on how the correlation functions of the classical system depend on time as parameters in the classical potential are varied, we may then determine the corresponding time-dependent correlation functions of the dual many-body quantum system. That is, we need not always find corresponding quantum systems to classical systems; the Fokker-Planck mapping also enables us to go in the opposite direction from quantum systems to classical ones.

Numerous related extensions may be considered. For instance, we may consider magnetic and other systems in which fermionic degrees can be formally integrated out, leaving only effective bosonic degrees of freedom. Consequences for the Ward identity relating four-point with two-point correlation functions (as in, e.g., Ref. 89) may be considered. The

Langevin equation may be reexamined for single vortex crossing of a narrow superconducting wire at finite temperature to derive the mapping for the quantum dual at absolute zero temperature.^{90,91} This would offer an alternative path for exploring the viability of quantum phase slips in nanowires.

ACKNOWLEDGMENTS

Z.N. thanks M. Alford, B. Altshuler, C. Bender, J. Cardy, S. Davis, S. Franz, V. Gurarie, A. Hamma, E.-A. Kim, A. Liu, S. Nagel, and C. Reichhardt for discussions and ongoing work. In particular, Sec. VIII was triggered by a question raised by E.-A. Kim and S. Davis. We thank C. Bender for a quick tutorial on aspects of Stokes’ wedges on which Appendix A heavily relies. Work at Washington University in St. Louis has been supported by the National Science Foundation (NSF) under Grant No. NSF DMR- 1106293. Research at the KITP was supported, in part, by the NSF under Grant No. NSF PHY11-25915. Z.N. also thanks Los Alamos National Laboratory (LANL) where a part of this work was done. Z.N. and A.V.B. further thank the Aspen Center for Physics for hospitality and NSF Grant No. 1066293. Work at LANL was carried out under the auspices of the NNSA of the U. S. DOE at LANL under Contract No. DE-AC52-06NA25396 through the Office of Basic Energy Sciences, Division of Materials Science and Engineering.

APPENDIX A: ANALYTIC CONTINUATION OF CLASSICAL STRETCHED EXPONENTIALS

In Sec. III B, we explicitly illustrated how a Wick-type rotation $t \rightarrow it$ relates time-dependent correlation functions in the viscous classical systems to those in the dual quantum many-body theories. For the sake of clarity, we explicitly discuss how the analytic continuation of the classical correlation function should be performed in some simple yet empirically relevant cases for dynamical response functions in viscous classical systems wherein Eq. (11) describes the dynamical response. In Eq. (12), we provided the quantum dual to exponentially stretched classical dynamics. In this brief Appendix, we describe how this result is derived and outline how analytic continuations for other response functions of classical viscous systems may be analytically continued following such a Wick-type rotation.

If $G_{\text{classical}}(t) = \sum_n B_n e^{-t/\tau_n}$ then, trivially, the quantum response function will be uniquely defined and given by $R_Q = \sum_n B_n \cos(t/\tau_n)$. The same applies, of course, for distributions of modes [whence the discrete sum over overdamped classical modes n is replaced by an integral with some density of modes $f(\tau)$]. In the limit of an infinite number of modes,

$$G_{\text{classical}}(t) = \int_0^\infty d\tau' f(\tau') \exp(-t/\tau'), \quad (A1)$$

with f a distribution that generally is no longer a sum of Dirac delta functions. As stated in Eq. (9), $G_{\text{Quantum}}(t) = G_{\text{classical}}(it)$. Thus,

$$G_{\text{Quantum}}(t) = \int_0^\infty d\tau' f(\tau') \exp(-it/\tau'). \quad (A2)$$

In the complex τ' plane, for any “well-behaved” function $f(\tau')$ that is localized in a region of positive finite τ' , the

integral of Eq. (A1) may be performed along any contour connecting the origin and the $\tau' = \infty$ along the real line such that the contour lies exclusively in the right half complex plane (the pertinent Stokes wedge in this case) of a positive real component of τ' , i.e., $\text{Re}\{\tau'\} \geq 0$. Of particular interest to us is the stretched exponential form given by $G_{\text{classical}}(t) = A \exp[-(t/\tau)^c]$. Now, in performing the substitution $t \rightarrow it$ to implement the transformation from Eq. (A1) to (A2), we perform the rotation

$$t = te^{i\varphi}, \varphi : 0 \longrightarrow \varphi_{\text{final}}, \quad (\text{A3})$$

with $\varphi_{\text{final}} = \pi(4n + 1)/2$ where n is an integer. The integral of Eq. (A2) remains well defined in the top complex half-plane of a positive real part of τ' , i.e., $\text{Re}\{\tau'\} \geq 0$ (the rotated counterpart of the original Stokes wedge). If φ is varied continuously from 0 to $\pi/2$, there remain contours from $\tau' = 0$ to ∞ that appear in the original Stokes wedge of $\text{Re}\{\tau'\} \geq 0$ that pass exclusively through the region $\text{Im}\{\tau'\} \geq 0$; the integrals along these contours can be analytically continued when φ is continuously increased from 0 to $\pi/2$. Thus, we may perform the rotation of Eq. (A3) continuously increasing φ to represent i as $e^{i\pi/2}$ and replace $t \rightarrow te^{i\pi/2}$ in the argument of $G_{\text{classical}}(t)$. This is what we have done in Eq. (12). For other choices of n for $\varphi_{\text{final}} = \pi(4n + 1)/2$ as we continuously vary φ from its initial value of zero, there will always appear situations where the original Stokes wedge will have no overlap with its rotated counterpart. Thus, the substitution of $t \rightarrow te^{i\pi/2}$ in the argument of $G_{\text{classical}}(t)$ is the only one that may be implemented out of the possible choices in Eq. (A3) in order to evaluate the integral of Eq. (A2). This forms the correct analytic continuation of the original real-time correlation function of $G_{\text{classical}}(t)$ of Eq. (A1).

APPENDIX B: RELATION BETWEEN THE CLASSICAL AND QUANTUM POTENTIALS IN THE EIKONAL APPROXIMATION TO THE SCHRÖDINGER EQUATION

Following, we briefly review the eikonal approximation and then discuss its relation to the connection between the classical and quantum many-body potentials as seen in Eqs. (7) and (28). This link lies at the heart of Madelung hydrodynamics.²⁹ Towards this end, we write the wave function as a function of only the phase, the eikonal approximation

$$\Psi_0 = Ae^{iS}, \quad (\text{B1})$$

and substitute this into the Schrödinger equation with the Hamiltonian in the second line of Eq. (7), then we will arrive at

$$\frac{1}{2m} \sum_i (\vec{\nabla}_i S)^2 + \mathcal{V}_{\text{Quantum}}(\{\vec{x}\}) + \frac{\partial S}{\partial t} = \frac{i}{2m} \sum_i \nabla_i^2 S. \quad (\text{B2})$$

For time-independent solutions, $\frac{\partial S}{\partial t} = 0$ and Eq. (B2) rather trivially becomes

$$\mathcal{V}_{\text{Quantum}}(\{\vec{x}\}) = \sum_i \left[\frac{i}{2m} \nabla_i^2 S - \frac{1}{2m} (\vec{\nabla}_i S)^2 \right]. \quad (\text{B3})$$

If we now invoke the correspondence $iS \leftrightarrow -\beta V_N/2$, then Eq. (B1) will transform into Eq. (28) and, similarly, Eq. (B3)

will become Eq. (7) relating the quantum potential energy $\mathcal{V}_{\text{Quantum}}$ to the classical potential energy V_N .

APPENDIX C: SIMPLE EXAMPLES OF CLASSICAL-TO-QUANTUM CORRESPONDENCE AND THEIR ASPECTS

To elucidate some aspects of the known mapping between classical dissipative and quantum systems reviewed in Sec. III A, we discuss several extremely simple examples in d spatial dimensions.

1. Noninteracting particles

For a (free) system having zero potential everywhere, the quantum ground-state wave function is a constant in real space. That this is so can be seen by our mapping and the form of the classical probability in Eq. (28) for vanishing classical potential energy. By Eq. (7), the same also occurs for the quantum potential, which is everywhere zero: $\mathcal{V}_{\text{Quantum}} = V_N = 0$.

2. Zero-energy bound state

In d spatial dimensions, for a short-range attractive potential, the zero-energy eigenstate outside the potential, up to volume normalization factors, is given by

$$\Psi_0(\vec{x}) = \frac{A}{|\vec{x}|^{d-2}}. \quad (\text{C1})$$

Invoking Eq. (28), we see that, in this case,

$$V_N^{\text{free}}(\{\vec{x}\}) = 2T_d(d-2) \ln |\vec{x}|. \quad (\text{C2})$$

Indeed, substituting Eq. (C2) into (7) and recalling that, in its scalar “ S -wave” (or “ $\ell = 0$ ”) representation, the Laplacian is given by $\nabla^2 = \frac{d^2}{dr^2} + \frac{d-1}{r} \frac{d}{dr}$, it is readily verified, as it must self-consistently be, that the corresponding quantum potential $\mathcal{V}_{\text{Quantum}} = 0$ in the region outside the range of the interaction.

3. Harmonic oscillator systems

As seen by Eq. (7), classical systems with harmonic potentials V_N map onto quantum systems with similar (up to innocuous shifts) harmonic potentials $\mathcal{V}_{\text{Quantum}} = V_N + \text{const}$. That this must be so is readily seen as the ground state Ψ_0 of simple quantum harmonic potentials is given by a Gaussian. Using Eq. (28), we see that this indeed relates to a harmonic classical potential V_N as it must. As can be further seen from Eq. (32), in the case of harmonic classical systems, the operators A and A^\dagger are trivially related to the raising and lowering operators in the quantum harmonic problem (and indeed the Gaussian form of the ground state can, as is very well known, be seen from the requirement that the annihilation operator must yield zero when acting on the ground state).

4. Scaling invariance of time and space

As is well known, for a homogeneous classical potential $V_N(\{\vec{x}\})$ which scales as a power (say, p) of the spatial coordinates $|\vec{x}|$, the equations of motion are invariant under a simultaneous rescaling of the time coordinates. This analysis

is typically done for inertial systems. When replicated for the overdamped system of Eq. (5), we find that

$$\vec{x}_i \rightarrow a\vec{x}_i, t \rightarrow bt, \quad (\text{C3})$$

where b plays the role of the scaling parameter λ discussed in the Introduction and a plays the role of $\lambda^{1/z}$. This leads to an invariance of Eq. (5) if $b = a^{2-p}$. By contrast, in the corresponding quantum problem of the Schrödinger equation with the Hamiltonian of Eq. (7), a scaling such as that of Eq. (C3) is possible only for a single case: that of a potential $V_N(\{\vec{x}\})$ that is a logarithmic function of its arguments (e.g., as in Eq. (C2)) or a constant. For this particular case, we find that $b = a^2$. Correspondingly, the time scales as $t \sim |x|^2$ as in diffusion or the free-particle quantum problem.

APPENDIX D: SLATER-JASTROW FORMS

The general results presented thus far may, in some instances, be generalized to describe fermions. A limited extension is the one concerning the evolution starting off from an initial Slater-Jastrow-type fermionic wave function. As we have emphasized earlier, if the V_{ij} in Eq. (62) are symmetric under the exchange of i and j , the resulting wave function obeys Bose statistics. This symmetry is maintained for the ground state as it is a Jastrow function given by Eq. (28). Fermionic wave functions are afforded by the product of the symmetric boson ground state and an antisymmetric term

$$\Psi_F = \Psi_0 \chi. \quad (\text{D1})$$

The function χ can take any antisymmetric form. For simplicity, we choose it to be a Slater determinant of the form

$$\chi = \frac{1}{\Omega^{N/2}} \frac{1}{\sqrt{N!}} \begin{vmatrix} e^{i\vec{k}_1 \cdot \vec{r}_1} & e^{i\vec{k}_1 \cdot \vec{r}_2} & \dots & e^{i\vec{k}_1 \cdot \vec{r}_N} \\ e^{i\vec{k}_2 \cdot \vec{r}_1} & e^{i\vec{k}_2 \cdot \vec{r}_2} & \dots & e^{i\vec{k}_2 \cdot \vec{r}_N} \\ \vdots & \vdots & \ddots & \vdots \\ e^{i\vec{k}_N \cdot \vec{r}_1} & e^{i\vec{k}_N \cdot \vec{r}_2} & \dots & e^{i\vec{k}_N \cdot \vec{r}_N} \end{vmatrix}, \quad (\text{D2})$$

with Ω the volume of the system.

$$\text{As } i\partial_t \Psi_0 = H \Psi_0,$$

$$i\partial_t(\Psi_0 \chi) = \chi(i\partial_t \Psi_0) + \Psi_0(i\partial_t \chi) = \chi [H + E_{\text{Slater}}] \Psi_0, \quad (\text{D3})$$

where E_{Slater} is the energy of the free-particle system described by χ and

$$H(\Psi_0 \chi) = (T_0 + \mathcal{V}_{\text{Quantum}})(\Psi_0 \chi). \quad (\text{D4})$$

The potential energy operator, in the second term, leads to $\chi(\mathcal{V}_{\text{Quantum}} \Psi_0)$. The kinetic energy operator T_0 generates three

terms of, respectively, the forms $\sum_a (\nabla_a^2 \chi) \psi^0$, $\sum_a (\nabla_a \chi) \cdot (\nabla_a \psi^0)$, and $\sum_a \chi (\nabla_a^2 \psi)$. The first and the last of these terms represent the term proportional to E_{Slater} and the original bosonic kinetic energy, respectively. The second term, that of the mixed gradients, is proportional to $\sum_a \vec{k}_a$. For a system invariant under parity, this sum vanishes. Up to an innocuous phase factor, the evolution given an initial fermionic wave function of Eq. (D1), will be thus identical to that with the bosonic wave function Ψ_0 and all correlation functions will be identical to those which we earlier computed for the bosonic system. That is, the general time-dependent correlation functions given an initial fermionic state of Eqs. (28) and (D1) will adhere to the general $t \rightarrow it$ rule, which we detailed in earlier sections. A notable difference by comparison to the bosonic case, however, is that the wave function of Eq. (D1) at an initial (or at a final) time is, generally, not a ground state of the Hamiltonian H .

APPENDIX E: COMPLEX WAVE FUNCTIONS

We now briefly suggest and elaborate on several extensions of our calculations thus far. We will illustrate and suggest how our results may hold for general systems with complex wave functions. This will enable us to go from a given quantum mechanical problem (including that of a fermionic system) to a corresponding classical one.

The similarity transformation of Eqs. (21), (27), and (29) captures a simple mathematical identity between the generalized probability distribution of a classical system, obeying the Fokker-Planck dynamics with an operator H_{FP} [Eq. (19)], and the wave function obeying the Schrödinger equation of the quantum dual Hamiltonian H . Given this relation, it is possible to, formally, consider extensions in which the function evolving with the Fokker-Planck dynamics need not be a probability distribution. Most of our results concerning temporal correlations may hold under such a generalized interchange if we invoke Eq. (28) to define (when given a quantum problem) a corresponding classical system which need not be a bona fide physical Boltzmann distribution as in the scalar bosonic systems which we primarily focused on thus far and employ $|\Psi_0|^2$ as the initial (or final) time weight in the multiple time classical correlation function of Sec. III B. In Appendix B, we examined a formally imaginary counterpart to V_N and explicitly demonstrated how it leads to standard results. Thus, given a quantum wave function, we may consider its logarithm to correspond to a classical potential V_N . Wave functions of spinless Fermi systems can not be purely positive, and for these complex (as well as divergent) potentials will formally arise. There may be subtleties, however, in our imaginary-time ($t \rightarrow it$) analytic continuations when V_N is not purely real (and the system effectively not purely dissipative) which are more complex than those which we invoked thus far in our analysis of real V_N , which led to response functions of pure damped modes and their superpositions such as those which we encountered in Eq. (11) (see also Appendix A). Physically, these are related to analogs of classical systems with instantons and tunneling events (the behavior for the pure dissipative system) when these further exhibit nondamped oscillatory behavior.

- ¹S. Sachdev, *Quantum Phase Transitions* (Cambridge University Press, Cambridge, UK, 2004).
- ²C. M. Varma, Z. Nussinov, and W. van Saarloos, *Phys. Rep.* **361**, 267 (2002).
- ³Y. S. Oh, K. H. Kim, P. A. Sharma, N. Harrison, H. Amitsuka, and J. A. Mydosh, *Phys. Rev. Lett.* **98**, 016401 (2007).
- ⁴Q. Si, S. Rabello, K. Ingersent, and J. Llewellyn Smith, *Nature* **413**, 804 (2001).
- ⁵M. J. Lawler and E. Fradkin, *Phys. Rev. B* **75**, 033304 (2007).
- ⁶V. Aji and C. M. Varma, *Phys. Rev. B* **82**, 174501 (2010).
- ⁷Z. Nussinov, C. D. Batista, B. Normand, and S. A. Trugman, *Phys. Rev. B* **75**, 094411 (2007).
- ⁸Z. Nussinov, I. Vekhter, and A. V. Balatsky, *Phys. Rev. B* **79**, 165122 (2009).
- ⁹J.-H. She, J. Zaanen, A. R. Bishop, and A. V. Balatsky, *Phys. Rev. B* **82**, 165128 (2010).
- ¹⁰A. Montanari and G. Semerjian, *J. Stat. Phys.* **125**, 23 (2006).
- ¹¹G. Biroli, J.-P. Bouchaud, A. Cavagna, T. S. Grigera, and P. Verrocchio, *Nat. Phys.* **4**, 771 (2008).
- ¹²H. Tanaka, T. Kawasaki, H. Shintani, and K. Watanabe, *Nat. Mater.* **9**, 324 (2010).
- ¹³M. J. Lawler *et al.*, *Nature (London)* **466**, 347 (2010).
- ¹⁴C. Panagopoulos and V. Dobrosavljevic, *Phys. Rev. B* **72**, 014536 (2005).
- ¹⁵Z. Nussinov, *Physics* **1**, 40 (2008).
- ¹⁶B. Olmos, I. Lesanovsky, and J. P. Garrahan, *Phys. Rev. Lett.* **109**, 020403 (2012).
- ¹⁷L. Berthier and G. Biroli, *Rev. Mod. Phys.* **83**, 587 (2011).
- ¹⁸S. F. Edwards and P. W. Anderson, *J. Phys. F: Met. Phys.* **5**, 965 (1975).
- ¹⁹C. Dasgupta, A. V. Indrani, S. Ramaswamy, and M. K. Phani, *Europhys. Lett.* **15**, 307 (1991).
- ²⁰G. Parisi, *Statistical Field Theory* (Frontiers in Physics, Addison Wesley, New York, 1988).
- ²¹J. Zinn-Justin, *Quantum Field Theory and Critical Phenomena* (Oxford University Press, Oxford, UK, 2002).
- ²²I. Fenyés, *Z. Phys.* **132**, 81 (1952).
- ²³E. Nelson, *Phys. Rev.* **150**, 1079 (1966).
- ²⁴F. Guerra and P. Ruggiero, *Phys. Rev. Lett.* **31**, 1022 (1973).
- ²⁵F. Guerra and L. M. Morato, *Phys. Rev. D* **27**, 1774 (1983).
- ²⁶G. Biroli, C. Chamon, and F. Zamponi, *Phys. Rev. B* **78**, 224306 (2008).
- ²⁷C. Castellano, C. Chamon, and D. Sherrington, *Phys. Rev. B* **81**, 184303 (2010).
- ²⁸M. V. Feigelman and M. A. Skvortsov, *Nucl. Phys. B* **506**, 665 (1997).
- ²⁹E. Madelung, *Z. Phys.* **40**, 322 (1926).
- ³⁰D. S. Rokhsar and S. A. Kivelson, *Phys. Rev. Lett.* **61**, 2376 (1988).
- ³¹Christopher L. Henley, *J. Phys.: Condens. Matter* **16**, S891 (2004); C. Castellano and C. Chamon, *Ann. Phys. (NY)* **318**, 316 (2005).
- ³²P. H. Damgaard and H. Huffel, *Phys. Rep.* **152**, 227 (1987); G. Parisi and Y.-S. Wu, *Scientia Sinica (Engl. Ed.)* **24**, 483 (1981).
- ³³J. M. Maldacena, *Adv. Theor. Math. Phys.* **2**, 231 (1998); *Int. J. Theor. Phys.* **38**, 1113 (1999); S. Gusber, I. R. Klebanov, and A. M. Polyakov, *Phys. Lett. B* **428**, 105 (1998); E. Witten, *Adv. Theor. Math. Phys.* **2**, 253 (1998); O. Aharony, S. S. Guber, J. M. Maldacena, H. Ooguri, and Y. Oz, *Phys. Rep.* **323**, 183 (2000); Z. Nussinov, G. Ortiz, and E. Cobanera, *Ann. Phys. (NY)* **327**, 2491 (2012).
- ³⁴W. T. Coffey, Y. P. Kalmykov, and J. T. Waldron, *The Langevin Equation: With Applications to Stochastic Problems in Physics, Chemistry, and Electrical Engineering* (World Scientific, Singapore, 2004); C. W. Gardiner, *Handbook of Stochastic Methods* (Springer, Berlin, 2004).
- ³⁵B. U. Felderhof, *Rep. Math. Phys.* **1**, 215 (1970); B. U. Felderhof and M. Suzuki, *Phys. (Amsterdam)* **56**, 43 (1971).
- ³⁶H. Risken, *The Fokker-Planck Equation* (Springer, Berlin, 1996), Chap. 6.
- ³⁷G. Junker, *Supersymmetric Methods in Quantum and Statistical Physics* (Springer, Berlin, 1996); M. O. Hongler and W. M. Zheng, *J. Stat. Phys.* **29**, 317 (1982); *J. Math. Phys.* **24**, 336 (1983); M. Bernstein and L. S. Brown, *Phys. Rev. Lett.* **52**, 1933 (1984); M. Hron and M. Razavy, *J. Stat. Phys.* **38**, 655 (1985); H. R. Jauslin, *J. Phys. A* **21**, 2337 (1988); M. J. Englefield, *J. Stat. Phys.* **52**, 369 (1988).
- ³⁸D. Forster, *Hydrodynamic Fluctuations, Broken Symmetry, and Correlation Functions* (Benjamin, New York, 1975).
- ³⁹D. N. Perera and P. Harrowell, *Phys. Rev. E* **59**, 5721 (1999).
- ⁴⁰W. Kob and H. C. Andersen, *Phys. Rev. Lett.* **73**, 1376 (1994); *Phys. Rev. E* **51**, 4626 (1995); O. Bang and M. Peyrard, *ibid.* **53**, 4143 (1996).
- ⁴¹Z. Rotman and E. Eisenberg, *Phys. Rev. Lett.* **105**, 225503 (2010).
- ⁴²H. Levit, Z. Rotman, and E. Eisenberg, *Phys. Rev. E* **85**, 011502 (2012).
- ⁴³G. Biroli and M. Mezard, *Phys. Rev. Lett.* **88**, 025501 (2001).
- ⁴⁴K. S. Cole and R. H. Cole, *J. Chem. Phys.* **9**, 341 (1941).
- ⁴⁵D. W. Davidson and R. H. Cole, *J. Chem. Phys.* **18**, 1417 (1950); **19**, 1484 (1951).
- ⁴⁶J. Rault, *J. Non-Cryst. Solids* **271**, 177 (2000).
- ⁴⁷D. R. Reichman and P. Charbonneau, *J. Stat. Mech.* (2005) P05013.
- ⁴⁸G. P. Johari and M. Goldstein, *J. Chem. Phys.* **53**, 2372 (1970).
- ⁴⁹M. Mierzwa, S. Pawlus, M. Paluch, E. Kaminska, and K. L. Ngai, *J. Chem. Phys.* **128**, 044512 (2008); K. L. Ngai, Z. Wang, X. Q. Gao, H. B. Yu, and W. H. Wang, arXiv:1303.7424 (2013).
- ⁵⁰C. Dreyfus, A. Le Grand, J. Gapinski, W. Steffen, and A. Patkowski, *Eur. Phys. J. B* **42**, 309 (2004).
- ⁵¹H. Sillescu, *J. Non-Cryst. Solids* **243**, 81 (1999); M. D. Ediger, *Annu. Rev. Phys. Chem.* **51**, 99 (2000); R. Richert, *J. Phys.: Condens. Matter* **14**, R703 (2002); W. Kob, C. Donati, S. J. Plimpton, P. H. Poole, and S. C. Glotzer, *Phys. Rev. Lett.* **79**, 2827 (1997); C. Donati, J. F. Douglas, W. Kob, S. J. Plimpton, P. H. Poole, and S. C. Glotzer, *ibid.* **80**, 2338 (1998); S. C. Glotzer, *J. Non-Cryst. Solids* **274**, 342 (2000); Y. Gebremichael, T. B. Schroder, F. W. Starr, and S. C. Glotzer, *Phys. Rev. E* **64**, 051503 (2001); J. X. Lin, C. Reichhardt, Z. Nussinov, L. P. Pryadko, and C. J. Olson Reichhardt, *ibid.* **73**, 061401 (2006).
- ⁵²M. E. Fisher, *J. Math. Phys.* **5**, 944 (1964).
- ⁵³K. Kim and S. Saito, *J. Chem. Phys.* **138**, 12A506 (2013).
- ⁵⁴S. Karmakar, C. Dasgupta, and S. Sastry, *Proc. Natl. Acad. Sci. USA* **106**, 3675 (2009).
- ⁵⁵R. P. A. Dullens and W. K. Kegel, *Phys. Rev. E* **71**, 011405 (2005).
- ⁵⁶M. Mosayebi, E. DelGado, P. Ilg, and H. C. Ottinger, *Phys. Rev. Lett.* **104**, 205704 (2010).
- ⁵⁷L. Berthier, G. Biroli, J.-P. Bouchaud, L. Cipelletti, D. El Masri, D. L'Hote, F. Ladieu, and M. Pierno, *Science* **310**, 1797 (2005).
- ⁵⁸J.-P. Bouchaud and G. Biroli, *J. Chem. Phys.* **121**, 7347 (2004).
- ⁵⁹J. Kurchan and D. Levine, arXiv:0904.4850.

- ⁶⁰E. Aharonov, E. Bouchbinder, H. G. E. Hentschel, V. Ilyin, N. Makedonska, I. Procaccia, and N. Schupper, *Europhys. Lett.* **77**, 56002 (2007).
- ⁶¹H. W. Sheng, W. K. Luo, F. M. Alamgir, J. M. Bai, and E. Ma, *Nature (London)* **439**, 419 (2006).
- ⁶²J. L. Finney, *Proc. R. Soc. London, Ser. A* **319**, 479 (1970).
- ⁶³J. Dana Honeycutt and Hans C. Andersen, *J. Phys. Chem.* **91**, 4950 (1987).
- ⁶⁴P. J. Steinhardt, D. R. Nelson, and M. Ronchetti, *Phys. Rev. B* **28**, 784 (1983).
- ⁶⁵P. Ronhovde, S. Chakrabarty, M. Sahu, K. F. Kelton, N. A. Mauro, K. K. Sahu, and Z. Nussinov, *Eur. Phys. J. E* **34**, 105 (2011); P. Ronhovde, S. Chakrabarty, M. Sahu, K. K. Sahu, K. F. Kelton, N. Mauro, and Z. Nussinov, *Sci. Rep.* **2**, 329 (2012).
- ⁶⁶R. Soklaski, Z. Nussinov, K. F. Kelton, Z. Markow, and L. Yang, [arXiv:1302.1895](https://arxiv.org/abs/1302.1895) (unpublished).
- ⁶⁷H. Mizuno and R. Yamamoto, *Phys. Rev. E* **84**, 011506 (2011).
- ⁶⁸A. J. Liu and S. R. Nagel, *Nature (London)* **396**, 21 (1998).
- ⁶⁹A. J. Liu and S. R. Nagel, *Annu. Rev. Condens. Matter Phys.* **1**, 347 (2010).
- ⁷⁰C. S. O'Hern, S. A. Langer, A. J. Liu, and S. R. Nagel, *Phys. Rev. Lett.* **88**, 075507 (2002).
- ⁷¹C. S. O'Hern, L. E. Silbert, A. J. Liu, and S. R. Nagel, *Phys. Rev. E* **68**, 011306 (2003).
- ⁷²J. A. Drocco, M. B. Hastings, C. J. Olson Reichhardt, and C. Reichhardt, *Phys. Rev. Lett.* **95**, 088001 (2005).
- ⁷³L. E. Silbert, A. J. Liu, and S. R. Nagel, *Phys. Rev. Lett.* **95**, 098301 (2005).
- ⁷⁴O. Dauchot, G. Marty, and G. Biroli, *Phys. Rev. Lett.* **95**, 265701 (2005).
- ⁷⁵A. R. Abate and D. J. Durian, *Phys. Rev. E* **74**, 031308 (2006).
- ⁷⁶A. R. Abate and D. J. Durian, *Phys. Rev. E* **76**, 021306 (2007).
- ⁷⁷A. S. Keys, A. R. Abate, S. C. Glotzer, and D. J. Durian, *Nat. Phys.* **3**, 260 (2007).
- ⁷⁸F. Lechenault, O. Dauchot, G. Biroli, and J.-P. Bouchaud, *Europhys. Lett.* **83**, 46003 (2008).
- ⁷⁹T. Hatano, *Phys. Rev. E* **79**, 050301(R) (2009).
- ⁸⁰J. Lidmar and M. Wallin, *Europhys. Lett.* **47**, 494 (1999).
- ⁸¹C. Reichhardt and C. J. Olson Reichhardt, *Phys. Rev. Lett.* **93**, 176405 (2004).
- ⁸²L. Berthier, H. Jacquin, and F. Zamponi, *Phys. Rev. E* **84**, 051103 (2011).
- ⁸³A. Ikeda, L. Berthier, and G. Biroli, *J. Chem. Phys.* **138**, 12A507 (2013).
- ⁸⁴Z. Zeravcic, N. Xu, A. J. Liu, S. R. Nagel, and W. van Saarloos, *Europhys. Lett.* **87**, 26001 (2009).
- ⁸⁵M. P. A. Fisher, P. B. Weichman, G. Grinstein, and D. S. Fisher, *Phys. Rev. B* **40**, 546 (1989).
- ⁸⁶G. T. Zimanyi, P. A. Crowell, R. T. Scalettar, and G. G. Batrouni, *Phys. Rev. B* **50**, 6515 (1994).
- ⁸⁷J. Schmalian and P. G. Wolynes, *Phys. Rev. Lett.* **85**, 836 (2000).
- ⁸⁸T. Matsubara and H. Matsuda, *Prog. Theor. Phys.* **16**, 569 (1956).
- ⁸⁹D. Belitz and T. R. Kirkpatrick, *Phys. Rev. B* **85**, 125126 (2012).
- ⁹⁰L. N. Bulaevskii, M. J. Graf, C. D. Batista, and V. G. Kogan, *Phys. Rev. B* **83**, 144526 (2011).
- ⁹¹L. N. Bulaevskii, M. J. Graf, and V. G. Kogan, *Phys. Rev. B* **85**, 014505 (2012).